

Aus dem Zentralinstitut für Seelische Gesundheit  
(Direktor: Prof. Dr. Andreas Meyer-Lindenberg)

# **Brain networks in pharmacological fMRI of NMDA antagonists**

Inauguraldissertation  
zur Erlangung des Doctor scientiarum humanarum (Dr.sc.hum.)  
der Medizinischen Fakultät Mannheim  
der Ruprecht-Karls-Universität  
zu  
Heidelberg

vorgelegt von  
Diplom-Physiker Robert Becker  
aus  
Wiesbaden  
2019

Dekan: Prof. Dr. med. Sergij Goerd  
Referent: apl. Prof. Dr. med. Dipl. Phys. Alexander Sartorius

# Contents

<b>1</b>	<b>Introduction</b>	<b>1</b>
1.1	Aims . . . . .	3
<b>2</b>	<b>Network methods in neuroscience</b>	<b>5</b>
2.1	Network definition . . . . .	5
2.2	Network analysis . . . . .	7
2.3	Studies . . . . .	13
<b>3</b>	<b>Study: Species-conserved reconfigurations of brain networks induced by Ketamine</b>	<b>15</b>
3.1	Abstract . . . . .	15
3.2	Introduction . . . . .	16
3.3	Methods . . . . .	17
3.4	Results . . . . .	23
3.5	Discussion . . . . .	26
3.6	Conclusions . . . . .	30
3.7	Supplementary Information . . . . .	30
<b>4</b>	<b>Study: NMDA receptor antagonists traxoprodil and lanicemine improve hippocampal-prefrontal coupling and reward related networks in rats</b>	<b>35</b>
4.1	Abstract . . . . .	35
4.2	Introduction . . . . .	36
4.3	Methods . . . . .	37
4.4	Results . . . . .	41
4.5	Discussion . . . . .	47
4.6	Conclusion . . . . .	51
4.7	Supplementary material . . . . .	51
<b>5</b>	<b>Discussion</b>	<b>55</b>
5.1	Establishment of network methods in preclinical studies . . . . .	55
5.2	Effects of NMDA antagonists on rat brain networks . . . . .	56
5.3	Limitations . . . . .	58

5.4	Future work . . . . .	58
5.5	Conclusion . . . . .	60
	<b>Summary</b>	<b>61</b>
	<b>Bibliography</b>	<b>63</b>
	<b>Curriculum Vitae</b>	<b>77</b>
	<b>Acknowledgements</b>	<b>81</b>

# 1

## Introduction

In the last two decades blood oxygenation level dependent (BOLD) functional magnetic resonance imaging (fMRI) has become a widely used tool in neuroscientific research. After the relation of neuronal activity and BOLD signal was discovered, fMRI was used to detect neuronal responses to various tasks compared to control periods during which the brain was considered inactive (Biswal, Zerrin Yetkin, Haughton, & Hyde, 1995). However, some regions of the brain were found to be active especially in this resting condition (Raichle et al., 2001). The discovery of the so called default mode network (DMN) evoked increasing interest in resting state investigations and resting state fMRI (rs-fMRI) has evolved into an active and fruitful field of research. Many studies have investigated alterations in resting state brain function induced by various abnormal conditions including psychiatric disorders and drug induced states. Rs-fMRI also provides the possibility to define networks on the level of brain regions, which can yield valuable information about functional processes in the brain.

In recent years, neuroscientists, especially in functional imaging, are increasingly regarding the brain as a complex network (Bassett & Sporns, 2017; Sporns, 2011; Bullmore & Sporns, 2009). Therefore, network scientific methods have

gained great popularity in neuroscience and are widely used in the field. Due to its high degree of abstractness the network representation allows for direct comparison between different studies and even different species.

Since preclinical MR scanners and sequences provide sufficient spatio-temporal resolution for functional imaging, there are more and more preclinical studies providing network results directly comparable to clinical studies or diagnostic data (Lu et al., 2012). Comparability of results across species is vital for translational research and the validation of animal models. Therefore, network methods appear to be especially useful in preclinical research. Direct comparison between human and animal studies can provide valuable results for validation of animal models. Nevertheless, studies directly comparing network results across species are rare.

In clinical research, psychiatric disorders are considered to be related to or even caused by disrupted brain networks (van den Heuvel & Hulshoff Pol, 2010; Braun, Muldoon, & Bassett, 2015), reflecting the connectomic view of the brain. Relating network phenotypes to clinical outcome could facilitate the definition of biomarkers quantifying psychiatric disorders as well as therapeutic success.

Major depressive disorder (MDD), one of the most prevalent psychiatric disorders, has been shown to affect functional connectivity and resting state networks in clinical studies as well as animal models (Mulders, van Eijndhoven, Schene, Beckmann, & Tendolkar, 2015; Q. Gong & He, 2015; Gass et al., 2016). There is considerable variation between studies due to the heterogeneity of the disease and differences in selection of patients (e.g. treatment resistance, medication). Nevertheless, there are results, including improved network integration and impaired reward processing, which keep recurring across studies (Q. Gong & He, 2015; L. Gong et al., 2017). Since brain networks are found to be altered in depression, network effects of antidepressant treatment are naturally an interesting target of investigation, especially in evaluating the effects and mechanisms of action of possible new antidepressants like ketamine.

Ketamine, an N-methyl-D-aspartate (NMDA) receptor antagonist, is a well established general anaesthetic, especially for use in emergency situations. Ketamine anaesthesia improves the outcome of electroconvulsive therapy in treatment resistant depression (Kranaster, Kammerer-Ciernioch, Hoyer, & Sartorius, 2011). Furthermore it was found to act antidepressantly at subanesthetic doses (Berman et al., 2000). Unlike classic antidepressants, like selective serotonin reuptake inhibitors (SSRI), ketamine was found to act very quickly. While SSRI usually need weeks to take full effect, ketamine significantly improves depressive symptoms within hours after a single injection (Diazgranados, Ibrahim, Brutsche, & et al., 2010; Zarate et al., 2006). Furthermore the antidepressant effect of ketamine is very reliable. Improvement of depression scores was found

across studies in unipolar and bipolar depression (McGirr et al., 2015) and even treatment-resistant patients responded to ketamine (Diazgranados et al., 2010). However the antidepressant effect comes at the price of dissociative side effects preventing a wider clinical usage of ketamine (Vollenweider & Komater, 2010). There is evidence suggesting that antidepressant and dissociative effects are based on the same neurochemical mechanisms (Niciu et al., 2018; Vollenweider & Komater, 2010). Regarding functional connectivity ketamine strengthens connections within the prefrontal cortex (PFC) as well as hippocampal-prefrontal coupling (Gass et al., 2014; Grimm et al., 2015). Whether these network effects reflect the antidepressant or the dissociative actions of ketamine is subject to ongoing investigation.

Since the antidepressant effect of ketamine has been discovered, there is increasing interest in NMDA antagonists in the research of antidepressant drugs. Alternative drugs could be found among compounds sharing ketamine's rapid antidepressant action without exhibiting strong side effects. There are results suggesting that ketamine's antidepressant action originates from its effect on the NR2B subtype of NMDA receptors (Miller et al., 2014). Therefore, antagonists exclusively targeting this subgroup are promising candidates for new antidepressant drugs. One compound belonging to this group is traxoprodil (CP101,606), which has shown antidepressant efficacy in clinical studies (Preskorn et al., 2008). Another candidate drug possibly showing this profile is lanicemine (AZD7665), an NMDA channel blocker with lower trapping than ketamine. In clinical studies it showed short lived antidepressant efficacy (Sanacora et al., 2014; Zarate et al., 2013).

Understanding the mechanism underlying both, the antidepressant and dissociative effects, is important for the development of glutamatergic antidepressants. Investigation and comparison of network effects induced by different NMDA receptor antagonists promises further insight into these mechanisms. Effects on the connectivity within the PFC as well as hippocampal-prefrontal coupling are especially interesting as differences between drugs might help understanding how network alterations induced by NMDA antagonists are related to antidepressant or dissociative effects.

## 1.1 Aims

One aim of this work is the translation of network methods, which are mostly applied in human studies, to preclinical research. Direct comparison of network effects across species is important for validation of the translational potential these methods have for pharmacological research as well as basic neuroscience.

In order to examine inter-species translatability of network methods, data obtained in resting state fMRI experiments studying the effects of ketamine on human and rat brains are analysed and results are compared across species (chapter 3). The hypothesis tested here is that ketamine induces similar network effects in both species.

Understanding the processes underlying the effects of NMDA antagonists is vital for the development of this new class of potential antidepressants. To that end, the acute actions of traxoprodil and lanicemine on networks in the rat brain are investigated in an exploratory study (chapter 4). Both drugs' effects on resting state connectivity and graph theoretical properties of brain networks are examined and compared to the effects of ketamine found in previous studies, which include increased connectivity in the hippocampal-prefrontal network (Gass et al., 2014) as well as reduced network integration and improved reward processing (Gass et al., 2018). Since clinical studies found antidepressant effects of ketamine and traxoprodil, network effects are hypothesised to be congruent as well. For lanicemine similar but less pronounced effects compared to ketamine are expected due to the similar mechanism of action.



# 2

## Network methods in neuroscience

### 2.1 Network definition

The basic idea of network science is to represent a system by a group of nodes connected by edges carrying certain weights representing the strength of connection. Legend has it that the birth of network science was Euler's consideration, whether there is a closed path through Königsberg which uses each of the bridges exactly once (Euler, 1736). Since then a branch of mathematics called graph theory has evolved, which provides a formalism for this kind of topological problems (Diestel, 2017).

In brain networks derived from fMRI measurements nodes are usually anatomically defined brain regions, provided by an atlas, e.g. the ones by Schwarz et al. (2006) for rats, or by J. Power et al. (2011) for humans. Edge weights are obtained by pairwise correlation of the mean regional BOLD time-courses (van den Heuvel & Hulshoff Pol, 2010). Figure 1 shows the network definition procedure schematically. As correlation is undirected ( $cor(A, B) = cor(B, A)$ ), a network of  $N$  regions contains  $\frac{1}{2}N(N - 1)$  edges.

While this is the most common definition, it is by far not the only one. For instance, some studies use widespread activation patterns obtained by independent component analysis (ICA) instead of anatomically defined regions as nodes (Jafri, Pearlson, Stevens, & Calhoun, 2008), some apply alternative measures of

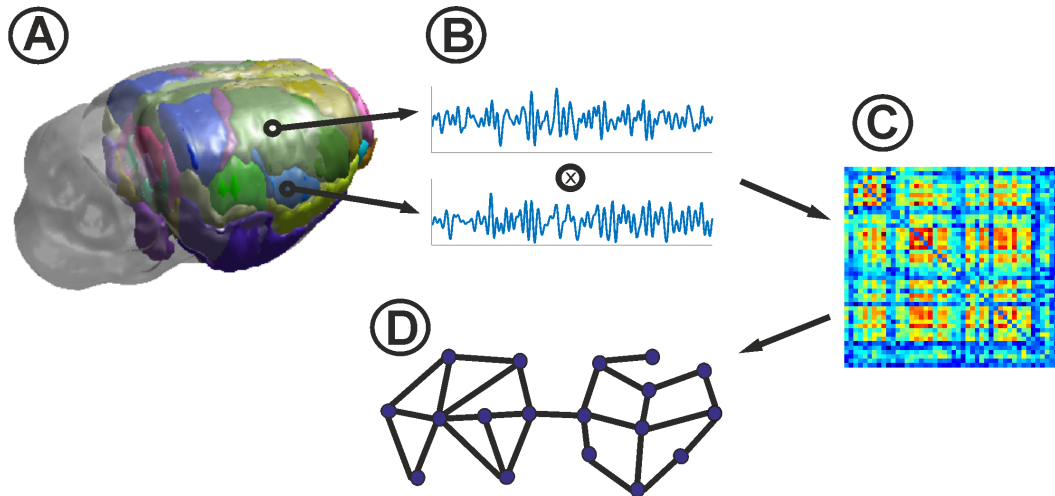


**Figure 1:** Definition of networks from rs-fMRI data. *A:* Brain parcellation by anatomical atlas; *B:* Pairwise correlation of regional timecourses; *C:* adjacency matrix with  $\frac{1}{2}N(N - 1)$  correlation coefficients. *D:* Sparse network for further analysis.

connectedness between regional signals like wavelet coherence (Grinsted, Moore, & Jevrejeva, 2004; Chai et al., 2017) or Granger’s causality (Bressler & Seth, 2011; Liao et al., 2011).

Formally a graph is defined by a set of nodes and a set of edges connecting them.

$$G = (V, U) \quad ,$$

where  $V$  is set of  $N$  nodes and a  $U$  a set of  $M \leq N(N - 1)$  edges.

A useful representation is an  $N \times N$ -matrix containing the connections of the edges. The adjacency matrix  $A$  gives the connection status of each pair of nodes:

$$a_{ij} = \begin{cases} 1, & \text{if nodes } i \text{ and } j \text{ are connected} \\ 0, & \text{otherwise} \end{cases}$$

If differently strong connections are allowed for, the weighted connectivity matrix  $W$  contains the weights  $w_{ij}$  of connections.

While consideration of the weights  $w_{ij}$  is essential in the analysis of connectivity, network topology can also be examined in the binary adjacency matrix  $A$ . Using weighted connections can unveil subtle topological changes, which are not detected by the binarized analysis, but possible interference of general connectivity changes and topological effects has to be accounted for.

## 2.2 Network analysis

Having defined a brain network, regional connectivity can be analysed, without calculating any higher level network metrics. Straight forward statistical methods like conventional parametric tests on the single network edges often yield interesting results in group comparisons (Gass et al., 2014). There are also more sophisticated methods available to analyse interregional connectivity. One widely used method is network based statistics introduced by Zalesky, Fornito, and Bullmore (2010). The basic idea of this approach is to compare connectivity at the level of clusters of nodes instead of analysing connections one by one. It is a translation of the known cluster based methods in statistical parametric mapping from the voxel to the network level. A conventional parametric test for the connections is performed and the network is sparsed by discarding all edges not exceeding an appropriate threshold value of the test statistic. In the thresholded network, connected subgroups are detected. Subsequently, group statistics are run with regard to these clusters, which leads to more robust results than classic statistics.

### 2.2.1 Network metrics

Apart from the analysis of connectivity itself, there is a large variety of network metrics which can yield information about network topology, which is not captured by the analysis of connectivity (Rubinov & Sporns, 2010; Sporns, 2011).

Nearly all approaches for network definition result in fully connected networks, i.e. every possible pair of nodes is connected. In order to get a meaningful and interpretable network it is necessary to sparsen the network. However, there is no consensus on which density to choose. In order to avoid arbitrarily choosing a single density, it is common to analyse networks over a range of densities and calculate the average values of network metrics, the area under the curve (AUC). Furthermore, there is no consensus on how to handle negatively weighted edges, as there is no conclusive interpretation and most network metrics can not be calculated for networks containing positive and negative weights. Therefore, the network analyses discussed in the following are restricted to networks consisting of positively weighted edges.

The selection of network metrics introduced here shall be mainly focused on those which are used for data analysis in chapters 3 and 4. Some network metrics are illustrated on an example network in Figure 2.

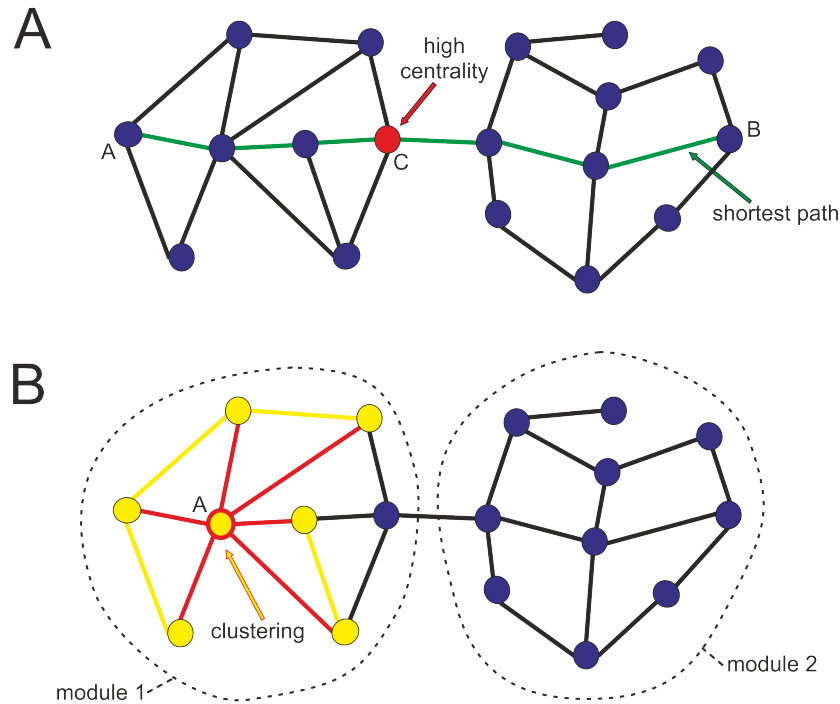


**Figure 2:** Illustration of some network metrics. **A:** Measures of integration, the edges shown in green form the shortest path between nodes A and B; node C (marked in red) is an example of a highly central node. **B:** Measures of segregation, clustering of node A is calculated based on the edges marked in yellow, which connect neighbours of A; the left and right halves of the network (dashed lines) are well separable modules.

### Basic metrics

The degree  $k$  of a node is the number of edges connecting it to others, and its strength  $s$  is the sum of weights of these connections:

$$k_i = \sum_{j \in V} a_{ij} ; \quad s_i = \sum_{j \in V} w_{ij} ,$$

where  $a_{ij}$  are the entries of the adjacency matrix  $A$  and  $w_{ij}$  the connection weights.

The distance between nodes  $i$  and  $j$  is given by the length of the shortest path connecting them (Watts & Strogatz, 1998; Rubinov & Sporns, 2010):

$$d_{ij} = \sum_{a_{uv} \in g_{i \leftrightarrow j}} \frac{1}{w_{uv}} ,$$

where  $g_{i \leftrightarrow j}$  is the shortest path between  $i$  and  $j$ ,  $w_{uv}$  the connection weights.

### Metrics of integration

Integration is the ability of a network to transfer information between any two nodes. Metrics of integration are based on the lengths of paths between nodes.

The characteristic path length of a network is the average shortest path length over all pairs of nodes, which are connected:

$$L = \frac{1}{N(N-1)} \sum_{\substack{i,j \in V, \\ i \neq j, a_{ij} \neq 0}} d_{ij} \quad ,$$

where  $N$  is the total number of nodes and  $d_{ij}$  the distance between nodes  $i$  and  $j$ .

An alternative metric of integration, the network's efficiency, is given by the average inverse shortest path length (Latora & Marchiori, 2001, 2003)

$$E = \frac{1}{N(N-1)} \sum_{\substack{i,j \in V, \\ i \neq j}} \frac{1}{d_{ij}} \quad ,$$

where  $N$  is the total number of nodes and  $d_{ij}$  the distance between nodes  $i$  and  $j$ .

Unlike the characteristic path length it can be meaningfully calculated on unconnected networks. Paths between non-connected nodes  $i, j$  have infinite length  $d_{ij} \rightarrow \infty$ , and do not contribute to the efficiency  $E$ , while they have to be explicitly excluded from calculation of the characteristic path length to avoid infinite values of  $L$  (note the additional restriction  $a_{ij} \neq 0$  in the calculation)

### Metrics of segregation

Segregation describes the ability of a network for localized processing. Highly segregated networks consist of highly connected, but separated subgroups and are therefore capable of processing information in parts of the network without disturbing others. This ability is also advantageous for many types of networks (Rubinov & Sporns, 2010; Sporns, 2011). Segregation can be quantified by the average clustering coefficient. A node's clustering coefficient is defined as the percentage of possible connections existing between its neighbours scaled by the edge weights:

$$C_i = \frac{1}{k_i(k_i-1)} \sum_{j,h \in N} (w_{ij}w_{ih}w_{jh})^{\frac{1}{3}} \quad ,$$

where  $k_i$  is the degree of node  $i$ ,  $w_{ij}$  the weight of the connection between nodes  $i$  and  $j$ .

The global clustering coefficient of a network is the average of the clustering coefficients of all its nodes.

$$C = \frac{1}{N} \sum_{i \in V} C_i$$

While the clustering coefficient is restricted to direct connections between the neighbours of  $i$ , the local efficiency also takes longer paths into account as long as they only contain neighbours of  $i$ . It is defined as the efficiency of the subnetwork formed by the neighbours.

$$E_{loc,i} = \frac{1}{k_i(k_i - 1)} \sum_{j,h \in N} (w_{ij}w_{ih}(d_{jh}(i))^{-1})^{\frac{1}{3}} \quad ,$$

where  $d_{jh}(i)$  is the distance between  $j$  and  $h$  only containing neighbours of  $i$ .

The local efficiency as a summary measure quantifying the segregation of the whole network is again given by the average of over all nodes:

$$E_{loc} = \frac{1}{N} \sum_{i \in V} E_{loc,i}$$

Another feature of segregation is the modular structure of a network. Modules are non-overlapping groups of nodes which have relatively high intrinsic connectivity, while being weakly connected to each other. The modularity  $Q$ , a measure of partition quality, is given by the average difference between within module connectivity of a given partition and within module connectivity expected by chance.

$$Q = \frac{1}{\nu} \sum_{ij} (w_{ij} - e_{ij}) \delta_{M_i M_j} \quad ,$$

where  $\nu = \sum_{ij} w_{ij}$  is the total weight of all edges,  $e_{ij} = \frac{s_i s_j}{\nu}$  the within-module connectivity expected by chance, and  $\delta_{M_i M_j} = 1$  if nodes  $i$  and  $j$  belong to the same module and  $\delta_{M_i M_j} = 0$  otherwise.

There are several algorithms available to find the optimal partitioning in numerical optimization processes maximizing  $Q$  (Newman, 2004; Blondel, Guillaume, Lambiotte, & Lefebvre, 2008).

### Small-world networks

Networks having high integration as well as high segregation are called small-world networks (referring to the known phenomenon of the world being smaller than we think)(Milgram, 1967; Watts & Strogatz, 1998). This structure can

be found in many real life networks like social communities, public transport or telecommunication (Latora & Marchiori, 2002; Guimerà, Mossa, Turtschi, & Amaral, 2005).

Brain networks are also supposed to show small-world structure (Bassett & Bullmore, 2006). The extent to which they do can be quantified by the small world index  $\sigma$ , which is given by the global clustering coefficient  $C$  divided by the characteristic path length  $L$  of the network:

$$\sigma = \frac{C}{L}$$

When compared to the small-worldness  $\sigma_{random}$  of a randomly structured network of the same size and density, the value of  $\sigma$  gives the extent of small-world topology. Small world networks are better segregated than random networks, while remaining similarly integrated, thus  $\frac{\sigma_{small-world}}{\sigma_{rand}} > 1$ .

### Centrality

Regarding the role of individual nodes in a network, their centrality is of interest. Metrics of centrality tell us how important a node is for a network's functionality. The simplest metric of centrality is the degree (see above).

A more sophisticated measure is the betweenness centrality index  $b_i$ , i.e. the fraction of shortest paths passing through a node:

$$b_i = \frac{1}{(N-1)(N-2)} \sum_{\substack{j,h \in V, \\ i \neq j, j \neq h, h \neq i}} \frac{\rho_{jh}(i)}{\rho_{jh}},$$

where  $\rho_{jh}$  is the number of shortest paths between  $j$  and  $h$ , and  $\rho_{jh}(i)$  the number of shortest paths between  $j$  and  $h$  passing through  $i$ .

### Network Motifs

Network motifs are small subnetworks, usually consisting of three or four nodes, which occur in a network (Sporns & Kotter, 2004; Onnela, Saramäki, Kertész, & Kaski, 2005). The frequency of occurrence of different motifs around a specific node, its motif fingerprint, yields information about the node's role in the network, e.g. closed circuit or cyclic motifs are reflecting high clustering and local processing whereas chain shaped motifs are associated with long-range connections and general integration. Depending on the topology of motifs occurring in the network in total, topological properties can be determined. A set of motifs suitable for the analysis of undirected networks is shown in Figure 3.

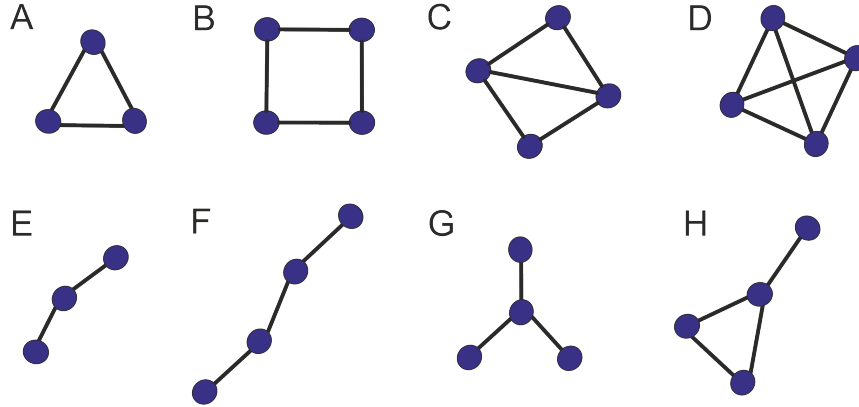


**Figure 3:** Set of 3 and 4 node motifs suitable for the analysis of undirected networks. A-D and H are cyclic motifs associated with network segregation, E-G are acyclic, integrative motifs

The intensity  $I_h$  of a motif  $h$  is given by:

$$I_h = \sum_{u \in U_h} \left( \prod_{(i,j) \in L_u^h} w_{ij} \right)^{\frac{1}{l_h}},$$

where  $U_h$  is the set of all occurrences of motif  $h$ ,  $L_u^h$  is the set of links in the  $u$ th occurrence of  $h$  and  $l_h$  the number of edges in motif  $h$ .

### Normalizing to randomized networks

In order to achieve comparability of network metrics between individual networks, it is necessary to normalize them by according metrics calculated on randomized networks. These randomized networks or null models are obtained by randomly redistributing the edges of the original network. Thereby the general structure of the network is maintained by preserving the distributions of degree and strength (Rubinov & Sporns, 2011). Since the randomized networks can vary significantly between runs, the outcome of many runs of the randomization process has to be averaged.



## 2.2.2 Image preprocessing

Before calculating networks, the raw fMRI recordings have to undergo some preprocessing. While there is no general consensus on which methods should be included in the preprocessing procedure, some of them can have considerable impact on the network outcome (Gargouri et al., 2018; Braun et al., 2012).

Especially the filtering of nuisance variables, mostly related to subject motion, breathing, and heartbeat from the fMRI data is considered important. The standard procedure of filtering motion related signal changes out of the fMRI timeseries is a linear regression of motion parameters directly obtained from the data during image realignment. But some researchers claim that this does not lead to sufficient removal of motion related signal and suggest more sophisticated methods. These include simply removing datapoints (“scrubbing”) based on motion detection methods like framewise displacement (FD) or DVARS (J. D. Power, Barnes, Snyder, Schlaggar, & Petersen, 2012; J. D. Power et al., 2014) or regressing additional data like externally recorded breathing and cardiac signals or more elaborate data driven methods like wavelet despiking (Patel et al., 2014) or ICA based methods. In the latter, the fMRI signal is decomposed into a number of components using independent component analysis (ICA) (Hyvärinen, Karhunen, & Oja, 2001). Then, components representing noise are discarded before reconstructing the data. Selecting those components which are considered noise by visual inspection is time consuming and prone to all kinds of bias the researcher classifying the components might be prone to. Therefore, automated component selection was developed by Pruim et al. (2015).

## 2.3 Studies

There have been numerous studies in the recent years which investigated network effects of many kinds of influencing factors including medication, psychiatric disorders on both interregional connectivity as well as the network metrics described above.

The network methods which were implemented in the course of this work have already been used in several studies by the research group Translational Imaging at the Central Institute of Mental Health. In a rat model of treatment resistant depression we found increased centrality along with reduced local efficiency for hubs of the DMN compared to stress resilient rats (Gass et al.,

2016). Optogenetic inhibition of the lateral habenula caused a reduction of DMN connectivity in the same animal model (Clemm von Hohenberg et al., 2018).

Examining the network effects of NR2B specific NMDA antagonists we found network effects opposite to those found in depressive patients (Gass et al., 2018). Like ketamine, traxoprodil induced decreased network integration and local alterations in several regions related to reward processing.

In socially isolated rats, a model of early life stress, we found reduced modularity of resting state brain networks as well as a shift of centrality from frontal to posterior regions (Reinwald et al., 2018).

In a study investigating effects of pain chronification in a mouse model of neuropathic pain we found a reduction in small-world structure as acute response one week after pain induction by spared nerve injury. Interestingly, network topology was reversed during pain chronification over the following 11 weeks (Bilbao et al., 2018).

# 3

## **Study: Species-conserved reconfigurations of brain networks induced by Ketamine**

This chapter was published in *Translational Psychiatry* in 2016 (Becker et al., 2016).

### **3.1 Abstract**

Species-conserved (intermediate) phenotypes that can be quantified and compared across species offer important advantages for translational research and drug discovery. Here, we investigate the utility of network science methods to assess the pharmacological alterations of the large-scale architecture of brain networks in rats and humans. In a double-blind, placebo-controlled, cross-over study in humans and a placebo-controlled two-group study in rats, we demonstrate that the application of ketamine leads to a topological reconfiguration of large-scale brain networks towards less-integrated and more-segregated information processing in both the species. As these alterations are opposed to those commonly observed in patients suffering from depression, they might indicate systems-level correlates of the antidepressant effect of ketamine.

## 3.2 Introduction

Ketamine, a potent N-methyl-D-aspartate (NMDA)-receptor antagonist, has spurred considerable interest in preclinical as well as clinical applications. Its effects range from anesthesia after acute application of high doses to psychomimetic symptoms, derealization and cognitive disruption (Anticevic et al., 2015; Höflich et al., 2015) as well as relatively rapid but long-lasting antidepressant action after acute administration of lower doses (Autry et al., 2011; Berman et al., 2000; Zarate et al., 2006). Furthermore, ketamine is widely studied in both human and laboratory animals as a translational pharmacological model of glutamatergic (dys-)function in schizophrenia (Anticevic et al., 2015; Gass et al., 2014; Inta, Sartorius, & Gass, 2015; Stone, 2009).

Several studies have probed the underlying neurobiological substrates of these actions in humans (Grimm et al., 2015; Höflich et al., 2015; Joules et al., 2015; Scheidegger et al., 2012; Scheidegger et al., 2016) and animals (Gass et al., 2014; Grimm et al., 2015; Lv et al., 2015) using neuroimaging approaches, but have largely focused on specific brain regions and their interactions. The first explicit demonstration of the translational potential of these methods showed altered prefrontal-hippocampal coupling after ketamine application in rats and humans, using a fMRI resting-state functional connectivity approach (Grimm et al., 2015).

However, given the ubiquity of NMDA receptors throughout the brain (Sanacora, Zarate, Krystal, & Manji, 2008), it is likely that ketamine modulates large-scale neural networks on the system-level, beyond alterations in single brain regions or specific circuits.

Developing translational biomarkers that are able to capture these global reconfigurations in a biologically meaningful way is a priority for drug research in psychiatry (Sanacora et al., 2008; Smucny, Wylie, & Tregellas, 2014). The application of network analysis in combination with task-independent brain imaging has been suggested as a key analytical tool, as network organization is closely linked to brain function (Sporns, 2011, 2013). Providing a formal representation of brain function, network analysis allows these fundamental neurobiological organizational principles to be quantified across species. Recent studies have successfully established graph theoretical metrics as reliable (Braun et al., 2012; Cao et al., 2014; Schwarz, Gass, Sartorius, Risterucci, et al., 2013; Schwarz & McGonigle, 2011) and sensitive biomarkers of normal (Bassett, Nelson, Mueller, Camchong, & Lim, 2012; Schwarz, Gozzi, & Bifone, 2009) and psychopathology-associated network function (Bassett et al., 2008; Bassett et al., 2012), both in humans and animals. Previous work also shows key network metrics to be conserved across species (Kaiser & Varier, 2011) and comparable

between biological neuronal networks and computers (Bassett et al., 2010), further suggesting that this approach may be useful for translational research and biotechnological development.

Our aim was to investigate how acute ketamine challenge modulates the topological characteristics of the brain-wide functional connectome in both rats and humans, and to assess the consistency of the large-scale network changes across species.

## 3.3 Methods

### 3.3.1 Subjects and ketamine application

Human fMRI data were acquired in 23 healthy individuals in a subject- and observer-blind, placebo-controlled, randomized three-period cross-over study, as previously reported (Grimm et al., 2015). Subjects were invited in a fixed interval of 7 days with each scanning session taking place at approximately the same time of day. Actual measurements took place with a mean interval of 7.7 days (SD: 2.5; range: 4 to 16 days). On each of three scanning visits, and approximately 60 min prior to the start of the MRI scan, subjects received intravenous cannulation followed by an infusion scan via a certified IV pump (Braun Medical, Melsungen, Germany). Subjects received counterbalanced single intravenous doses of either saline (placebo condition), ketamine (0.5 mg/kg body weight) or scopolamine ( $4\mu$  g/kg body weight) following previously published protocols (Furey, Khanna, Hoffman, & Drevets, 2010; Salvadore et al., 2010). All study participants and personnel involved in the experiments were blind to the respective substance given. Individual doses of ketamine hydrochloride were adjusted to body weight (0.5 mg/kg) following previously published protocols (Diazgranados et al., 2010), diluted in saline, and applied over 40 min. The placebo condition consisted of a 40-min saline infusion. During the infusion, subjects were seated comfortably in chair under supervision of a board certified psychiatrist. To avoid order effects, the sequence of substance applications was randomly permuted across all 23 participants. MRI scanning took place after drug administration, with the resting-state measurement starting approximately 20 min after the end of the infusion. The data from the scopolamine challenge were not analyzed for the current report.

All participants provided written informed consent for the study approved by the local ethics committee (Medical Faculty Mannheim, University of Heidelberg, Germany). A total of 23 participants completed the study (11 female, mean age  $25.13 \pm 2.51$  years, mean body weight  $70.24 \pm 11.56$  kg, mean height

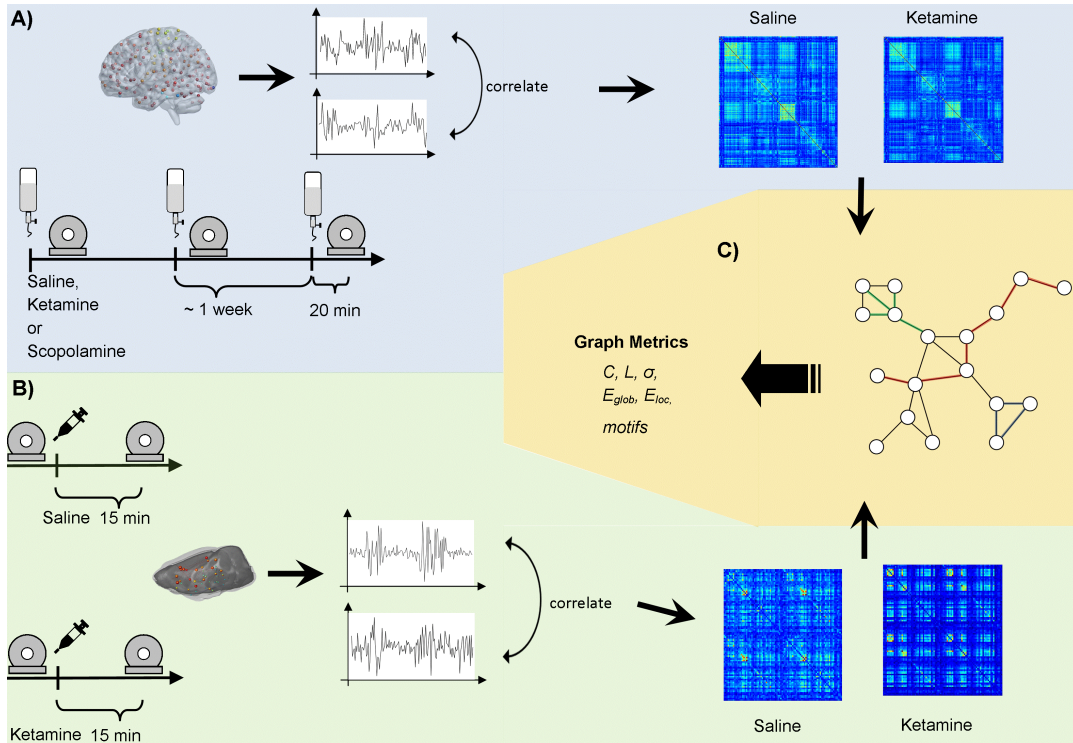


**Figure 4:** Study protocols and methods. (a) Human (light blue): the subjects received either saline, ketamine or scopolamine via infusion over 45 min, 20 min before each scanning session. BOLD fMRI resting-state data were acquired and the time series of 270 brain regions were extracted. Correlated, these yielded two correlation matrices for each subject. (b) Rats (light green): the two groups of animals received either ketamine or saline injection. BOLD resting-state data were acquired before and 15 min after the injection. The time series of 90 brain regions were extracted and correlated, resulting in one correlation matrix for each animal. (c) Both human and animals matrices were thresholded and binarized to extract the underlying topological network structure. Subsequently, graph metrics such as degree (green lines in the depicted network), path length (red lines) and clustering coefficient (blue) were computed.

1.75  $\pm$  0.80 meters, mean Body-Mass-Index 22.76  $\pm$  2.71). One subject that initially participated was excluded from the study, as she was not able to complete all 3 required MRI measurements.

As this was an exploratory study, no formal power or sample size estimation was performed. The group size was selected based on prior experience and literature reports of pharmacological-fMRI studies in healthy subjects, and is toward the high end of the range of sample sizes typically used.

### 3.3.2 Animals and ketamine application

18 Sprague-Dawley male rats (weight: 373-447 g, age 10-11 weeks; Janvier Laboratories, Le Genest-St-Isle, France) were used for fMRI experiments. Animals were housed under controlled conditions (19-23°C, 40-60% humidity) with a 12:12 h light-dark cycle (lights on at 7 a.m.).

All procedures were performed according to the regulations covering animal experimentation within the European Union (European Communities Council Directive 86/609/EEC) and within the German Animal Welfare Act and were approved by the German animal welfare authorities (Regierungspräsidium Karlsruhe). The rat rs-fMRI data were originally analyzed using a seed-based approach, the results of which have been reported elsewhere (Gass et al., 2014). As that study was exploratory in nature, no formal power or sample size estimation was performed, but the group sizes (N=9 per group) are toward the high end of the range typically used in rat fMRI experiments. The exploratory nature of the experiment was explicitly mentioned in the discussion section of (Gass et al., 2014) No blinding was done, since for the given type of experiment it is not possible: ketamine solution had to be prepared before each experiment depending on the dose.

The experimental design comprised two groups of N=9 rats each. In one group, S-ketamine (Ketanest<sup>®</sup>, Pfizer Pharma GmbH, Berlin, Germany) was injected subcutaneously at a dose of 25 mg/kg dissolved in saline (total volume 1 ml/kg). The second group received the same volume of vehicle (saline). The rats were assigned to the groups randomly. The order of ketamine and saline injections was randomized across animals and time of day. fMRI resting-state measurements were acquired immediately before and starting at 15 min after the ketamine/vehicle injection.

These animals represent two groups from the study previously reported (Gass et al., 2014). The 25 mg/kg group was selected for the present analysis as it yielded plasma concentrations closest to those obtained in the human study (Grimm et al., 2015). The rat data were re-analyzed using methods as closely aligned as possible to those used for the human data (see Fig.1).

### 3.3.3 Data acquisition and preprocessing - human fMRI

BOLD fMRI was acquired at a 3 Tesla MR scanner (Siemens TIM-Trio, Erlangen, Germany), with the Syngo MR VB17 Software, max. 45 mT/m (z-axis) and 40 mT/m (x- and y-axis) gradient strength, a 32-channel head-coil, and an echo-planar imaging (EPI) sequence with full brain coverage with the following parameters: TR = 1790 ms, TE = 28 ms, 34 oblique slices (aligned to the AC-

PC plane) in descending acquisition order, 3 mm slice thickness, + 1 mm gap, flip angle =  $76^\circ$ , FoV = 192 mm, 64x64 matrix, 3x3 mm in-plane voxel size, and 332 volumes. Preprocessing of functional data consisted of slice time correction, realignment, and smoothing by a 6mm FWHM Gaussian kernel (FSL 5.0.6) followed by noise correction with the AROMA framework (Pruim et al., 2015). In short, this includes removal of noise related independent by means of an automated detection of noise components based on their time course correlation with movement parameters as well as their high frequency fraction and the overlap of their maps with brain edges and CSF maps (for details see Pruum et al. (2015)). Data were afterwards corrected for nuisance covariates of WM and CSF signal as well as the 6 motion parameters obtained during realignment (Pruim et al., 2015). Data were finally normalized to MNI standard space EPI template (SPM8). 264 whole-brain functional nodes were extracted from 5mm spheres around coordinates defined by Power et al. (J. Power et al., 2011). Since the Power atlas does not cover the hippocampus, amygdala and nucleus accumbens, we included additional six bilateral nodes of interest based on meta-analytical data (Liu, Hairston, Schrier, & Fan, 2011; Sabatinelli et al., 2011; Spreng, Mar, & Kim, 2018). In a final step, each node's time-series was bandpass filtered at a frequency range of 0.01 to 0.15 Hz.

### 3.3.4 Data acquisition – rat fMRI

Experiments were conducted at a 9.4 Tesla MRI scanner ( 94/20 Bruker BioSpec, Ettlingen, Germany) with Avance III hardware, BGA12S gradient system with the maximum strength of 705 mT/m and Paravision 5.1 software. Transmission and reception were achieved using a linear whole-body volume transmitter coil combined with an anatomically shaped 4-channel receive-only coil array for the rat brain.

Rats were anesthetized under 4% isoflurane (Baxter Deutschland GmbH, Unterschleissheim, Germany) in a mixture of N<sub>2</sub>(70%)/O<sub>2</sub>(30%). After positioning in the scanner (head first, prone), 2.5% isoflurane was provided for adjustments. Then, a bolus of 0.5 ml medetomidine solution (Domitor<sup>®</sup>, Janssen-Cilag, Neuss; 0.07 mg/kg s.c.) was administered; isoflurane was slowly discontinued within the next 10 min, after which a continuous infusion of medetomidine solution started at 0.14 mg/kg/h rate.

Breathing and cardiac signals were monitored using a respiration pad placed beneath the chest (Small Animal Instruments Inc., NY, USA) and a pulse oximeter attached to the hindpaw, respectively. A signal breakout mod-



ule (Small Animal Instruments Inc., NY, USA) and a 4-channel recorder (Velleman<sup>®</sup> N.V., Gavere, Belgium) were used to record signals (10-ms resolution).

The MRI acquisition protocol for each animal comprised a Field Map and a rs-fMRI measurement. To acquire the rs-fMRI time series, an echo-planar imaging (EPI) sequence was used with the following parameters: repetition time/echo time (TR/TE) 1700/17.5 ms, flip angle 60°, 1 segment, 29 coronal slices (ascending slice order), 96x96 imaging matrix, field of view 35x35 mm<sup>2</sup>, slice thickness 0.5 mm with 0.2 mm inter-slice gap, in-plane voxel dimension 0.365 mm, 300 acquisitions over 8.5 min. The slice stack covered the brain from the cerebellum to the posterior olfactory bulb.

The preprocessing of the data included correction for field inhomogeneities (SPM8), regression of movement parameters (FSL, version 4.1), filtering of respiratory and cardiac signals (Aztec (van Buuren et al, 2009)), slice timing correction (SPM8) and band pass filtering (0.01 to 0.1 Hz, using Analysis of Functional NeuroImages (AFNI) software). Additionally the images were spatially normalized (SPM8) to a rat brain template with co-registered atlas in the Paxinos stereotactic coordinate system (Schwarz et al, 2006) and finally the signal from CSF was filtered out. A single time-series was extracted for each of 90 anatomically defined ROIs (Schwarz et al, 2006) by averaging single-voxel time-series over all voxels in a ROI.

### 3.3.5 Network analysis – humans and rats

Brain networks for humans and rats were constructed by computing the Pearson correlation coefficient between the time series extracted from each pair of regions of interest. The correlation coefficients were transformed to Fisher-Z-scores. Subsequently, networks were created by binarizing these correlation matrices. As there is no current consensus on the selection of network density (fraction of all possible links that is actually present), we computed all graph metrics over a range of densities (0.05 to 0.2 in steps of 0.01 – for details see supplemental material) as previously described (Braun et al., 2012; Cao et al., 2014; Lv et al., 2015; J. Power et al., 2011). The selection of density thresholds was led by two methodological considerations. On the one hand we wanted our analysis to be sensitive to subtle alterations in network topology. Due to the large number of possible connections and the relatively small number of connections actually being different under ketamine, a threshold beyond 0.2 would significantly impair this sensitivity. On the other hand, given the high degree

of network fragmentation (i.e. the number of disconnected nodes) at lower densities, we choose a density of 0.05 as the lowest cut-off to ensure a reasonable degree of connectedness.

This procedure normalizes all networks to have the same number of links and removes the effect of global differences in correlation strength. Standard network parameter computation was implemented in MATLAB, using the Brain Connectivity Toolbox (BCT) (Rubinov & Sporns, 2010). For each subject and each density level we computed the following network parameters: clustering coefficient, characteristic path length, small-worldness, and global and local efficiency. Details on the computation and interpretation of the specific graph metrics can be found in the supplemental material.

Furthermore we calculated the networks' motif frequencies, also using functions implemented in BCT, for a sequence of 8 motifs consisting of (undirected) connections of three to four nodes.

### 3.3.6 Network Based Statistics – humans and rats

While network analysis can detect changes in the topological organization of brain networks, we also aimed to test for global differences in absolute connectivity. To that end, we used the Network Based Statistics (NBS) toolbox (Bullmore & Sporns, 2009; Rubinov & Sporns, 2010) to identify alterations in specific connections after ketamine application. The NBS deals with the multiple comparison correction for tests by evaluating the null hypothesis on the level of connected subcluster rather than individually for each connection. Using a corrected p-level of 0.05, we report the largest connected subclusters identified by NBS.

### 3.3.7 Statistical analysis and hypothesis testing

Instead of testing each metric at each density level, we calculated the area under the curve (AUC) for each metric, motif frequency and subject. This yields density summary estimators for each network metric and avoids the still unresolved question of multiple comparison correction in modern network analysis (Achard, Salvador, Whitcher, Suckling, & Bullmore, 2006). Subsequently, we tested the AUCs of each metric using paired and independent sample t-tests. For comparisons in humans a paired t-test was conducted, whereas independent two-sample t-tests were used for the rats since they consisted of two different groups. All reported p-values are  $<0.05$ , FDR corrected for multiple comparisons unless otherwise specified.

## 3.4 Results

### 3.4.1 Alterations of network metrics by ketamine in humans

After application of ketamine, human brain networks showed a decrease in global and local efficiency compared to placebo ( $p_{FDR} < 0.05$ ), as well as a decrease in the small-world coefficient ( $p_{FDR} < 0.05$ ). An increase of the characteristic path length was found only as trend ( $p = 0.08$ ). Further, ketamine induced a significant increase of cyclic motifs ( $p_{FDR} < 0.05$ ), while the acyclic motifs were not significantly altered (see 5, 6).

### 3.4.2 Alterations of network metrics by ketamine in rats

After application of ketamine, the brain networks of rats showed an increase in clustering coefficient compared to placebo ( $p_{FDR} < 0.05$ ), as well as an decrease in the average path length ( $p_{FDR} < 0.05$ ). This is reflected in the decrease global efficiency ( $p_{FDR} < 0.05$ ). Sigma, the small-world coefficient also decreased ( $p_{FDR} < 0.05$ ). As in humans, networks after ketamine showed an increased abundance of cyclic motifs ( $p_{FDR} < 0.05$ ), but further a significant decrease of acyclic motifs (see Figures 5, 6).

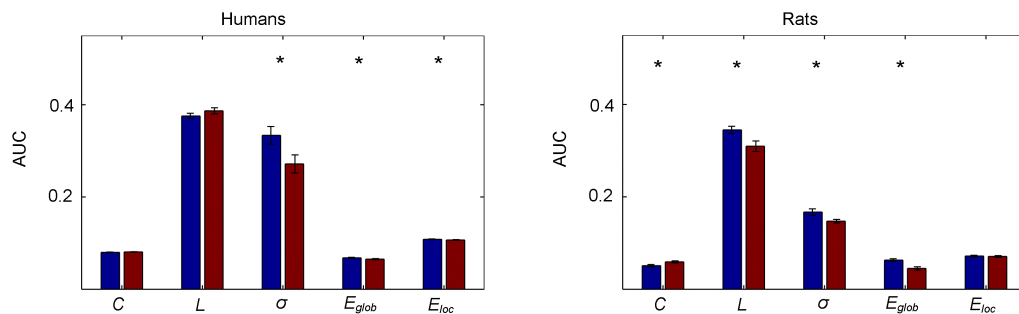


**Figure 5:** Topological reconfigurations after ketamine application. Means of area under curve (AUC) for each calculated graph metrics for humans (a) and rats (b) after saline application (blue) and ketamine (red). Asterisks denote statistically significant differences ( $p < 0.05$ , FDR corrected) between saline and ketamine. C, clustering coefficient;  $E_{glob}$ , global efficiency;  $E_{loc}$ , local efficiency; FDR, false discovery rate; L, path length;  $\sigma$ , small-worldness coefficient.

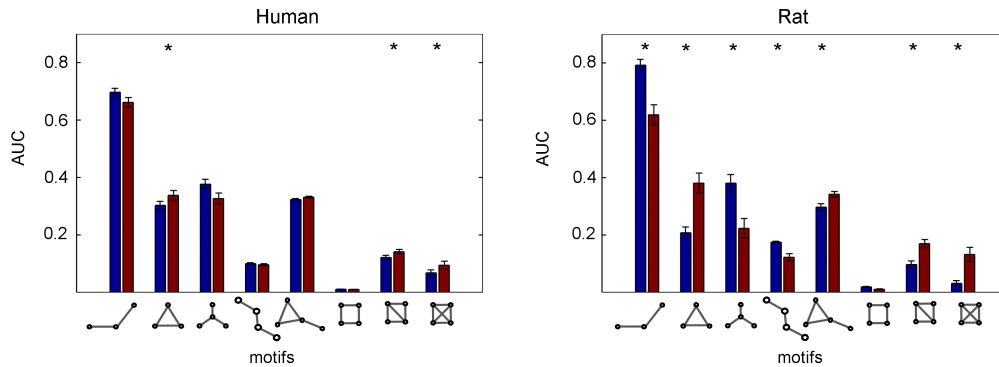


**Figure 6:** Area under curves of network motif frequencies for undirected three- and four-node motifs. For both humans (a) and rats (b), red bars indicate mean values for the ketamine groups, and blue bars indicate mean values for the controls; asterisks denote statistically significant differences between the groups ( $p < 0.05$ , FDR corrected). AUC, area under the curve; FDR, false discovery rate.

To provide further evidence that the observed group differences between saline and ketamine conditions were indeed induced by the drug challenge (and are not driven by accidental differences between both groups), we repeated our analysis in both groups before applications of either ketamine or saline. As expected, we could not detect any difference between groups in any graph metric (all  $p > 0.5$ , see Figure 8).

### 3.4.3 Alterations of functional connectivity by ketamine in humans

NBS revealed a subnetwork consisting of 24 nodes and 24 increased connections with a T statistic of  $T > 4.4$  induced by infusion of ketamine ( $p_{corrected} < 0.05$ ). This subnetwork predominantly comprised regions of the frontal cortex ( $\sim 38\%$ ), parietal cortex ( $\sim 33\%$ ), as well as occipital (17%) and temporal cortex ( $\sim 13\%$ ). To further illustrate the importance of specific brain areas to the large scale reconfiguration observed before, we evaluated the number of altered connections for each node (see Figure 7). Two frontal areas, namely frontal superior medial cortex and the middle frontal cortex as well as the mid cingulate cortex exhibited the highest number of altered connections, identifying them as being prominently involved in ketamine-induced reconfigurations of brain networks.

### 3.4.4 Alterations of functional connectivity by ketamine in rats

A subnetwork of 31 edges with a T statistic of  $T > 5.1$  and 21 nodes was identified in rats after ketamine application ( $p_{corrected} < 0.05$ ). Increased connections could be mainly detected in infralimbic, prelimbic and orbital regions of the frontal cortex as well as the insular cortex (see Figure 7). Several cingulate and somatosensory areas also showed increased connectivity. The largest changes in number of connections occurred in the frontal and insular cortices. As in humans, the frontal cortex was most strongly affected by ketamine-induced network reconfiguration.

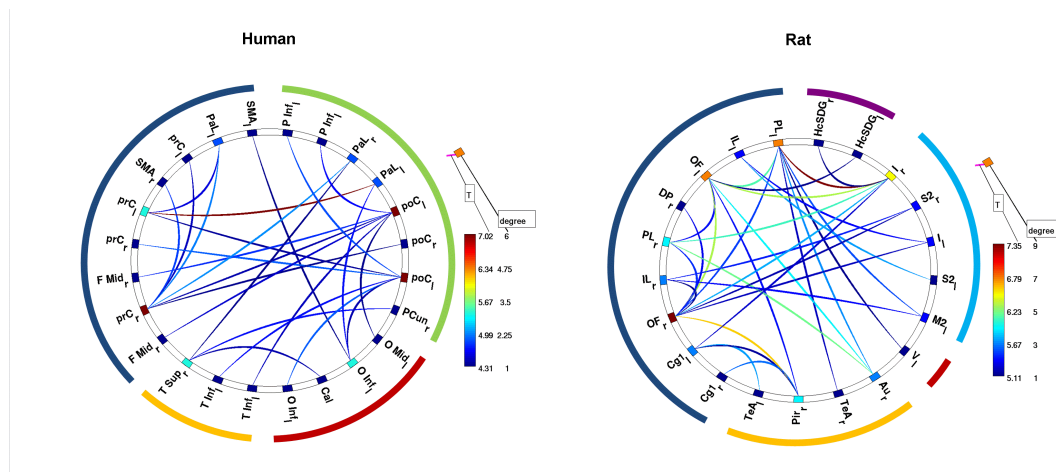


**Figure 7:** Alterations of functional connectivity after ketamine application. Ketamine-related increase in connectivity in humans (left) and rats (right). The line color represents the statistical significance as indicated by the respective T-statistics. The color of nodes indicates the number of altered connections for the respective node. The outer colored circle represents the brain region's assignment: blue=frontal cortex, yellow=temporal, red=orbital cortex, green=parietal cortex, magenta=hippocampal formation. The areas colored in lighter blue stretch along an anterior-posterior axis compassing multiple brain regions. Human: Cal, calcarine sulcus; F Mid, frontal middle cortex; O Inf, occipital cortex inferior sulcus; O Mid, occipital cortex middle sulcus; PaL, paracentral lobule; PCun, precunes; poC, postcentral sulcus; prC, precentral sulcus; SMA, supplemental motor area; T inf, temporal cortex inferior sulcus; T sup, temporal cortex superior sulcus. Rat: Au, auditory cortex; Cg1, cingulate cortex; HcSDG, hippocampus subiculum/dentate gyrus; I, insular cortex; IL, infralimbic cortex; M2, secondary motor cortex; OF, orbitofrontal cortex; Pir, piriform cortex; PL, prelimbic cortex; S2, secondary somatosensory cortex; TeA, temporal association area; V, visual cortex. Subscript indicates left (l) or right (r) hemisphere.

## 3.5 Discussion

Human and rat brains, despite all their differences, have shown some remarkable similarities in the spatial, functional and topological characteristics of intrinsic network architecture (Kaiser & Varier, 2011; Schwarz, Gass, Sartorius, Zheng, et al., 2013; Schwarz, Gass, Sartorius, Risterucci, et al., 2013). Network analysis has been proposed as a promising tool for translational neuroscience and especially cross-species drug discovery (Smucny et al., 2014), but studies utilizing the translational power of these approaches (De Vico Fallani, Richiardi, Chavez, & Achard, 2014; Smucny et al., 2014) are rare.

Here, we used network analysis to study the global topological reconfiguration of human and rat brain networks in response to a pharmacological challenge with sub-anaesthetic doses of ketamine.

### 3.5.1 Consistent reconfiguration of brain networks in humans and rats

After ketamine infusion, brain networks in both humans and rats showed an increase in overall connectivity, consistent with the results from previous studies (Anticevic et al., 2015; Driesen et al., 2013; Khalili-Mahani et al., 2015). In both species, the frontal cortex showed particularly prominent connectivity changes, which may be related to our previous findings of altered prefrontal-hippocampal connectivity (Grimm et al., 2015). Regarding the other affected brain regions, between-species concordance was incomplete. However, it should be noted that NBS is suitable for identifying cluster-wide connectivity changes, not for making inferences on specific connectivity pairs. This precludes detailed interpretation of the individual regions displaying altered connectivity in our data.

The connectivity increase was accompanied by a topological reconfiguration of large-scale brain networks towards a conformation characteristic of less integrated and more segregated information processing, as evidenced by decreases in global efficiency and a decrease in small-worldness. A higher abundance of cyclic motifs points towards a network organization more tuned to local processing and less suitable for efficient long range communication in both species. This is further supported by the decreased occurrence of acyclic motifs in rats, although this finding wasn't significant in humans. In line with a previous study using a different imaging modality, cross-animal correlations rather than within-subject temporal correlations and a different NMDA receptor antagonist (Dawson et al., 2014), we observed a loss of small-worldness properties after ketamine injection. Our study therefore adds further support to the idea of a compromised functional integration in NMDA receptor dysfunction mod-

els of disease. It is interesting to note that a previous study from our group using the same human and rat data as in the current work reported an increased prefrontal-hippocampal coupling after NMDA receptor blockade to be a cross-species phenotype altered by ketamine (Grimm et al., 2015).

Although a direct statistical comparison between species would be misguided for several reasons, the placebo-controlled design of both studies enabled us to compare findings between species qualitatively. Overall, we found highly concordant and directionally consistent network reconfiguration in humans and rats. In both species we observed an increased total connectivity. Topologically we detected a less globally integrated and more segregated network architecture following ketamine administration.

### 3.5.2 Discrepant findings in humans and rats

Interestingly, while motif analysis revealed a significant increase of cyclic motifs after ketamine infusion in both species, we found no difference in the clustering coefficient in humans. This might be a consequence of triangles being introduced primarily around nodes with a high degree, for which the clustering coefficient is less sensitive due its normalization by the number of all possible triangles.

Surprisingly, in rats we observed a decrease in path length after ketamine application, contrasting with effects on other parameters indicating a less integrated network architecture. However, this might be a result of our focus on sparsely connected networks, which often suffer from a higher fragmentation to which the characteristic path length (in contrast to global efficiency) is very prone.

### 3.5.3 Relation to mental disorders

Interestingly, the network reconfigurations identified here are opposite to network alterations in depressed patients, who show increased global efficiency and small-worldness compared to healthy controls (Q. Gong & He, 2015; Zhang et al., 2011). We hypothesize that this may indicate a network mechanism supporting the action of ketamine as rapidly acting antidepressant. This idea is further supported by a previous study showing ketamine effects on network topology opposite to those observed in depressed subjects (Lv et al., 2015).

Studies investigating brain network properties in schizophrenia consistently report reduced total connectivity as well as higher integration (e.g. increased local efficiency, decreased characteristic path length) and less local processing (e.g. decreasing clustering coefficient and local efficiency) (Braun et al., 2015; Fornito, Zalesky, Pantelis, & Bullmore, 2012). These findings are in contrast

to the observed network reconfigurations in our data, suggesting that acute ketamine application rather resembles a different glutamatergic state than observed in chronic schizophrenia.

### 3.5.4 Limitations

Despite our efforts to align protocols of the human and rat studies, there still remain some differences. First, ketamine was applied differently – subcutaneous bolus injection in rats versus intravenous continuous infusion in humans – and therefore might evoke different biological responses. Further studies are urgently needed, as application protocols might explain clinically diverse effects and could account for the heterogeneous results in previous human (Driesen et al., 2013; Scheidegger et al., 2012) and rat (Gass et al., 2014) studies. Second, in rats anesthesia as well as interactions of the anesthetic agent with ketamine might also influence the behavior of brain networks, although previous studies have shown a high correspondence of human and rat functional brain networks (Bähner et al., 2015; Grimm et al., 2015). A further potential limitation results from the different number of nodes used in humans and rats. However, by choosing a proportional thresholding approach, we aimed at examining changes in network architecture independent of the absolute number of links in a given network. Due to the thresholding approach our results are specific to the chosen range of network densities (5% to 20%) which surely is not the only possible choice of densities. Along with network size the composition of nodes is a possible restriction to comparability. While in humans 90% of the nodes are cortical, in rats the fraction is considerably smaller (40%), which reflects the substantially developed and differentiated cortex in humans. Despite this asymmetry in the fraction of cortical nodes, the results in both species can be compared thanks to the placebo-controlled design of the study in both species. We compare changes in network organization qualitatively rather than absolute quantities of network metrics in both species. Moreover, a closer look at the brain regions which experience most significant change in connectivity and number of connections reveals that in rats as well as humans effects of ketamine occur (almost) exclusively in cortical regions (see Fig 4). Another potential confound is the influence of the CBF increase induced by ketamine (Långsjö et al., 2003). The BOLD signal correlation changes we observed could include contribution from CBF increase per se or the differences in correlation may be modulated by CBF increase. Regrettably we did not measure CBF independently and therefore cannot access its impact on network results. Given the promising results on ketamine effects on functional connectivity in this study (and others in recent literature), further studies examining the effect of CBF are recommended.



Finally, while the animal study had a two-group design, the human study was designed as a placebo-controlled double-blind cross-over study. The missing control for between-subject variance in the animal study might account for the observed higher differences in rats, but a comparison between groups before ketamine applications revealed no differences between network parameters (see supplemental material).

### **3.5.5 Relevance for translational research and drug discovery**

These findings are encouraging for translational research and its application to drug discovery. The use of global brain parameters reflecting functional network topology has the advantage of reducing complex, high-dimensional imaging data to a few summary measures, reducing the multiple comparisons burden and avoiding the need to pre-specify specific brain regions or connections. The latter is valuable, and the involvement of specific brain systems is important to increase biological understanding, but can be difficult to apply with confidence, especially when dealing with novel compounds or mechanisms. Global brain network parameters may thus represent a more robust endpoint for translational functional imaging at the early phase of drug discovery and development. Importantly, the similarities in the pharmacological effects across species suggest that preclinical experiments can be used to inform early clinical phase biomarker studies. That said, the differences in the observed effects serve as a reminder that effects in humans are unlikely to be a perfect simulacrum of those observed in preclinical setting. This observation is consistent with other recent translational pharmacological imaging studies, where consistency between rodent and human effects was high but not complete (Becerra et al., 2013).

Another important caveat is that ketamine is a highly psycho-active compound. Novel compounds being developed as potential medicines are unlikely to induce such strong subjective effects per se, and their effects on brain functional connectivity may be more subtle. The sensitivity of network topology measures to a broader range of compounds and mechanisms remains to be established. However, as a pharmacological model of a hyperglutamatergic state, ketamine-induced changes in functional connectivity may serve as an example of brain function perturbation that can be reversed by pre-treatment with compounds of interest (Doyle et al., 2013; Joules et al., 2015). Finally, the sensitivity of results to methodological aspects such as brain parcellation scheme, image post-processing variations, choice of connectivity metric and thresholding or weighting scheme remains an important area of investigation.

## 3.6 Conclusions

Using network analysis and task-independent brain imaging, we observed highly concordant cross-species topological reconfigurations of large scale brain networks induced by acute ketamine administration in rats and humans. These changes indicated a pharmacologically-induced shift towards a more segregated, less integrated network conformation, and are opposite in valence to network topology changes observed in depressed subjects.

In conclusion, our results demonstrate the potential of these novel techniques for the identification of translational biomarkers for drug discovery.

## 3.7 Supplementary Information

### 3.7.1 Methods

#### Threshold selection

As there is no current consensus on how to select network thresholds in graph theoretical analysis, we chose the network density as the threshold according to previous studies (1-4). In short, each connectivity matrix was thresholded over a range of densities, taking into account only the respective percentage of absolute highest correlations or links. The choices of the density range (5% to 20% of the connections) was determined by two methodological considerations: i) given the high number of possible connections (for humans:  $270 \times 269 / 2 = 36315$ ; rats:  $90 \times 89 / 2 = 4005$ ), we wanted to be sensitive enough to subtle alterations. If, for example as in our human dataset, about 400 connections are different between conditions, at a density of 20% ( $= 7236$  absolute connections) only  $(400 / 7236 \times 100 = )$  5% of the considered connections are altered. Therefore, increasing the density beyond 20% would significantly impair our ability to detect topological difference between conditions. ii) given the high degree of network fragmentation (i.e. the number of disconnected nodes) at lower densities, we choose a density of 5% as the lowest cut-off to ensure a reasonable degree of connectedness.

#### Network-based Statistics

Network-based statistic (NBS) was used to identify clusters of functional links that are altered after applications of Ketamine. NBS is a method to effectively control cluster-level family-wise error (FWE) for link-wise matrical comparisons and offers a larger power than mass-univariate tests on independent links (5,

6). Consistent with prior studies (5-8), we applied initial directed paired t-tests for the human data to each of the  $N(N-1)/2 = 36315$  ( $N=270$ ) links in the connectivity matrices and initial directed t-tests for the rat data to each of the  $N(N-1)/2 = 4005$  ( $N = 90$ ) links in the connectivity matrices respectively, thereby generating a P-value matrix representing the probability of accepting the null hypothesis for each link.

All links with T-statistics of  $T > 4.4$  (humans) and  $T > 5.1$  were then thresholded into a set of suprathreshold links (8), and connected clusters within this set were identified by breadth first search (9). The significance of the identified clusters was tested by permutation testing, where i) sessions were randomly attributed for each subjects in the human dataset, and ii) in the rat dataset, the rats were randomly reallocated into one of the two groups and the maximal size of the identified cluster was recalculated during each of the 5000 permutations. The corrected P value for the cluster was determined by the proportion of the derived cluster sizes in the permutation distribution that were larger than the observed group difference.

### **Statistical analysis**

Prior to inference analysis, we thoroughly tested if our data met the assumptions of the tests (e.g., normal distribution) using the Kolmogorov-Smirnov Test for normality. As all test revealed no significant violation of the normality assumption, we subsequently proceeded using parametric tests (see Table 1). Further, equal variance was tested by Levene's test for inequality. If not satisfied, p-values for the non-equal variances estimates are reported.

## **3.7.2 Results**

### **Group differences in rats before substance application**

To show that the observed group differences between saline and ketamine conditions are indeed induced by the drug challenge (and are not driven by differences between both groups), we repeated our analysis of both groups before applications of either ketamine or saline (see Figure 8). As expected, we could not detect any difference between groups in any graph metric (all  $p > 0.5$ , see Figure 8).

**Table 1:** *p*-values for the comparisons Kolmogorov-Smirnov test for normality

	Humans	Rats	
		placebo	ketamine
clustering	0.977	0.995	0.352
path length	0.842	0.713	0.689
sigma	0.443	0.719	0.179
Eglob	0.800	0.255	0.935
Eloc	0.607	0.936	0.927
motif_31	0.697	0.564	0.787
motif_32	0.351	0.476	0.994
motif_41	0.580	0.360	0.917
motif_42	0.872	0.643	0.560
motif_43	0.980	0.996	0.961
motif_44	0.985	0.935	0.660
motif_45	0.713	0.801	0.831
motif_46	0.207	0.340	0.998

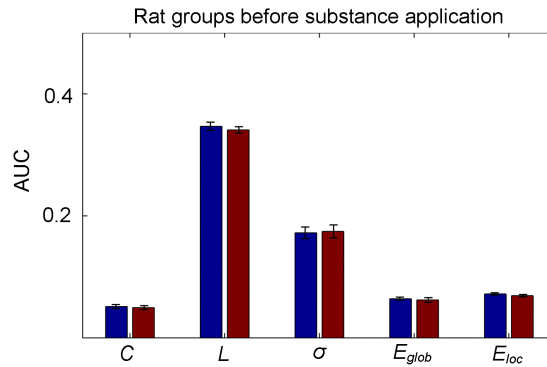


**Figure 8:** Comparison of graph metrics in both rat groups before application of saline or ketamine. No difference between the saline (blue) and ketamine (red) group could be detected for any of the tested graph metrics. All  $p > 0.5$  before corrections for multiple comparisons.

### Effects of bandpass filter

To increase comparability between species, we repeated our analysis of the human fMRI data with exactly the same bandpass filter used in the animals ((0.01 to 0.1 Hz). We found only marginal effects on the observed reconfiguration pattern induced by Ketamine on brain networks (see Table 2 and Figure 9).

**Table 2:** *p*-values for the comparisons of areas under the curve for the tested network metrics. Asterisk (\*) indicates significance after correction for multiple comparisons using the false discovery rate

Network metric	Animals (0.01-0.1 Hz)	Humans (0.01-0.15 Hz)	Humans (0.01-0.1 Hz)
Clustering coefficient	$p = 0.0249$ *	$p = 0.2925$	$p = 0.4963$
Path length	$p = 0.0208$ *	$p = 0.0896$	$p = 0.0566$
sigma	$p = 0.0249$ *	$p = 0.0042$ *	$p = 0.0047$ *
Global efficiency	$p = 0.0013$ *	$p = 0.0189$ *	$p = 0.0148$ *
Local efficiency	$p = 0.7336$	$p = 0.0241$ *	$p = 0.0310$

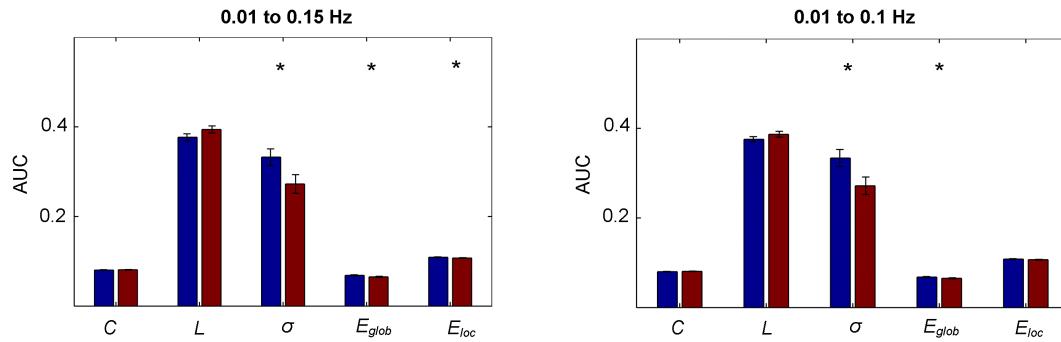


**Figure 9:** Comparison of graph metrics in humans after saline and ketamine for different frequency bands. Area under curves for each calculated graph metrics for humans with a bandpass filter of 0.01 to 0.15 Hz (A) and 0.01 to 0.15 Hz (B) after saline application (blue) and ketamine (red). Asterisks denote statistically significant differences ( $p < 0.05$ , FDR corrected) between saline and ketamine.  $C$  = clustering coefficient,  $L$  = path length,  $\sigma$  = small-worldness coefficient,  $E_{glob}$  = global efficiency,  $E_{loc}$  = local efficiency.

### Effect of age

To explore the impact of age on the observed network reconfiguration induced by ketamine, we correlated the differences in AUCs between saline and ketamine with age.

In humans, we could not detect any significant correlation with age (all  $p > 0.25$ , all  $r < 0.25$ ), with either Pearson and Spearman correlation.

### Additional NBS analyses

For each group, we first assessed the connectome differences by using a simple FDR correction approach as implemented in the NBS toolbox. In humans, we found 215 significant edges at a FDR-corrected p-level of 0.05, 212 edges at a FDR-corrected p-level of 0.01 and 157 edges FDR-corrected p-level of 0.001. Analogous, in rats, we found 248 significantly different edges at a FDR-corrected p-level of 0.05, 120 edges at a FDR-corrected p-level of 0.01 and 120 edges at a FDR-corrected p-level of 0.001.

To find a set of interpretable edges, we then systematically explored the connectomic difference starting with an initial T-threshold of  $T > 3.5$  in human and rats. This yielded 187 significantly different edges in rats and 206 edges in human, respectively. The last significant T-threshold could be identified as being  $T > 7.3$  in rats with one connections survived at  $p = 0.006$  and  $T > 4.5$  in humans with 6 edges surviving correction at a p-level of 0.042.

# 4

## **Study: NMDA receptor antagonists traxoprodil and lanicemine improve hippocampal-prefrontal coupling and reward related networks in rats**

This chapter was submitted for publication to *Neuropsychopharmacology* and is currently under review (Becker et al., submitted).

### **4.1 Abstract**

The N-methyl-d-aspartate receptor (NMDAR) antagonists traxoprodil and lanicemine are candidate antidepressant drugs with fewer side effects than ketamine. In order to understand their mechanism of action, we investigated their acute effects on brain connectivity using resting-state functional magnetic resonance imaging (rs-fMRI).

Functional connectivity (FC) alterations were examined using interregional correlation networks. Furthermore, graph theoretical methods were used for analysis of whole brain FC networks. As the interest in NMDAR antagonists as potential antidepressants was triggered by the antidepressant effect of ketamine, results were compared to previous findings from ketamine studies. Similarly to ketamine but to a smaller extent, traxoprodil increased hippocampal-prefrontal (Hc-PFC) coupling. Unlike ketamine, traxoprodil decreased connectivity within the prefrontal cortex (PFC). Lanicemine had no effect on these properties. Connectivity changes overlapping between the drugs as well as alterations of local network properties occurred mostly in reward related regions.

The improvement of Hc-PFC coupling corresponds well to clinical result, showing ketamine to have a greater antidepressant effect than traxoprodil, while lanicemine has a weak and transient effect. Thus, it can be concluded that the antidepressant effect of NMDA antagonists at least partly originates from enhanced hippocampal-prefrontal coupling. The effects on local network properties and regional connectivity suggest that improvement of reward processing might also be important for understanding the mechanisms underlying the antidepressant effects of these drugs.

## **4.2 Introduction**

The non-selective, non-competitive NMDA receptor antagonist ketamine has a rapid antidepressant effect, even in treatment resistant patients, if continuously applied at low doses for 45 min, iv (Berman et al., 2000; Zarate et al., 2006). However, its antidepressant action comes at the price of dissociative side effects which prevent a broader clinical use of ketamine (Vollenweider & Kommer, 2010). Alternative antidepressant drugs with fewer side effects could possibly be found among other NMDA receptor antagonists.

Lanicemine (AZD6765) is a low-trapping channel blocker inducing channel closure while it is bound to a site inside the channel (Mealing, Lanthorn, Murray, Small, & Morley, 1999). The degree of trapping correlates with the severity of side effects: the higher the trapping, as in e.g. ketamine (86% of trapping), the more severe the side effects. Lanicemine exhibits 54% of trapping and has an improved safety profile (Mealing et al., 1999). It produces rapid but transient antidepressant efficacy (Zarate et al., 2013), as well as sustained antidepressant effect after repeated administration (Sanacora et al., 2014), both without psychotomimetic or dissociative side effects.



Traxoprodil (CP-101,606) is a negative allosteric modulator of the NR2B subtype NMDAR. There is evidence that the antidepressant effect of ketamine is caused by its action on the NR2B-containing NMDAR (Miller et al., 2014). Thus, drugs exclusively antagonizing the NR2B subunit of NMDAR could be promising candidates for new antidepressants. Traxoprodil has rapid antidepressant effects with nearly no dissociative reactions with efficacy lasting for  $\approx$  1 week (Preskorn et al., 2008).

Two candidate drugs are examined in this study with regard to their effects on functional brain connectivity and network organisation, using rs-fMRI, as in recent years psychiatric disorders including depression are increasingly seen as disorders of the functional connectome (Artigas et al., 2017; Braun et al., 2015; Q. Gong & He, 2015; Sporns, 2011). Despite the differences caused by the heterogeneity of the disease and variations in the patient groups, there are results recurring across studies including improved network integration and impaired connectivity of reward related regions (L. Gong et al., 2017; Q. Gong & He, 2015). Rs-fMRI is widely used for investigation of functional changes induced by pharmacological challenges. Whole brain functional networks are a useful representation for detection and comparison of drug effects across studies and species (Becker et al., 2016; Gass et al., 2018; Gass et al., 2014; Grimm et al., 2015; Tang et al., 2018).

We aimed for results comparable to those of previous studies on ketamine, which found increased hippocampal-prefrontal as well as intra-PFC connectivity along with reduced network efficiency and small-worldness (Becker et al., 2016; Gass et al., 2014; Grimm et al., 2015). Considering that ketamine shows greater antidepressant effect than traxoprodil or lanicemine in clinical studies, we expected to find similar but less pronounced effects.

## 4.3 Methods

### 4.3.1 Animals

82 male Sprague-Dawley rats were used in this study. Animal experiments were conducted following the regulations of the European Union (European Communities Council Directive 86/609/EEC) as well as the German Animal Welfare Act and were approved by the responsible authorities (Regierungspräsidium Karlsruhe).

### 4.3.2 Drugs

Traxoprodil and lanicemine were provided by Boehringer Ingelheim Pharma, Ingelheim, Germany. The doses were selected in order to achieve 0.3, 1 and 3 times the exposure measured in clinical studies of traxoprodil (Johnson, Shah, Jaw-Tsai, Baxter, & Prakash, 2003; Preskorn et al., 2008; Taylor et al., 2006) and lanicemine (Guo, Zhou, Grimm, & Bui, 2015; Sanacora et al., 2014).

**Table 3:** Concentrations of drug solutions, target doses, and group sizes.

	Concentration (mg/ml)	Dosage (mg/kg)	Number of animals
Traxoprodil	0.52	1.04	11
	1.7	3.4	11
	5.2	10.4	11
Lanicemine	0.6	1.2	13
	2	4	12
	6	12	13
Control	-	-	11

Since the essential quantity for comparable effect size is the unbound plasma concentration of the compound, differing plasma protein binding (PPB) between humans and rats had to be accounted for. For lanicemine the PPB in rats was found to be higher than in humans (47% vs. 33%). Using clinical pharmacokinetic data and pharmacokinetic measurements conducted in rats, the temporal development of plasma concentrations of the drugs was simulated by pharmacokinetic modelling. PK model development and parameter estimation was performed using Phoenix WinNonlin 6.4, NLME 1.3 (Certara, Princeton, New Jersey, USA). Built upon these investigations, the concentrations necessary for comparable exposures in rats 40 minutes after subcutaneous injection were determined.

The actual dosage of the drugs followed from the volume of 2 ml/kg injected during each measurement. The concentrations, the according doses, and the group sizes are shown in 3.

The control group received the 2 ml/kg volume of the vehicle substance, dimethyl sulfoxide (DMSO).

### 4.3.3 Resting-state fMRI

MRI measurements were performed on a 9.4 T small animal scanner (Bruker Biospec, Avance III hardware, Paravision 6 software, Bruker Biospin, Ettlingen, Germany). Before each fMRI measurement a T2-weighted structural image (RARE,  $TR/TE = 1200/50ms$ , 0.15 mm isotropic resolution) and a fieldmap (double gradient echo,  $TR = 20ms$ ,  $TE = 1.7ms/5.7ms$ ) were recorded.

For each animal a 50 min fMRI was recorded (EPI sequence  $TR/TE = 1500/17.5ms$ , 0.365mm in plane resolution, 0.5 mm slice thickness). Drugs were injected 10 min after the beginning of each fMRI measurement. Thus, after a 10 min baseline period the fMRI scan covered 40 min post-injection for examination of acute drug effects.

Respiratory and cardiac signals were acquired using a respiration pad placed beneath the chest (Small Animal Instruments, Stony Brook, NY, USA) and a pulse oximeter attached to the hind paw, respectively. During the fMRI measurement these signals were recorded (100 Hz sampling rate) for later use in data processing.

We applied the same anesthesia protocol as in previous studies (Gass et al., 2018; Gass et al., 2014). Anesthesia was initiated by 4% isoflurane (Baxter Deutschland, Unterschleissheim, Germany), then maintained at 2.5%, 30 min before the beginning of the EPI, a bolus of medetomidine (Domitor, Janssen-Cilag, Neuss, Germany) was injected (0.07 mg/kg s.c.) and isoflurane was slowly discontinued. Stable sedation was ensured by continuous infusion of medetomidine (0.28 mg/kg/h, s.c.).

### 4.3.4 Image preprocessing

Data preprocessing included realignment, unwarping, slice time correction (SPM), filtering of respiratory and cardiac signals (Aztec (van Buuren et al., 2009)), RETROICOR (Glover, Li, & Ress, 2000)).

For correction of artifacts related to subject movement, we used an approach based on independent component analysis (ICA) (Hyvärinen et al., 2001), which has been previously used for denoising fMRI data (Kelly et al., 2010). We chose an automatized approach to distinguish noise from non-noise components similar to ICA-AROMA (Pruim et al., 2015). Finally, the data were bandpass-filtered in the range of 0.01 Hz to 0.1 Hz (AFNI).

### 4.3.5 ROI-ROI connectivity

Average regional time courses were extracted from the preprocessed data. Forty-six regions were defined using the rat brain atlas by Schwarz et al. (2006). All calculations were performed using MATLAB unless stated otherwise.

In order to achieve optimal comparability to a previous study on ketamine (Gass et al., 2014), we extracted three blocks of 400 time points (600 sec) each from the whole series of 2000 time points (3000 sec): one from the beginning of measurement (before drug injection) and two more 15 and 30 min after injection, respectively. For each set of regional time courses, ROI-ROI connectivity matrices were calculated as pairwise Pearson's correlation coefficients leading to three connectivity matrices per measurement. In order to examine changes in functional connectivity induced by the drug injection, we calculated difference matrices between both post-injection and pre-injection matrices for each subject. The effects of drug dosage and post-injection delay were investigated by two-way ANOVA using drug dosage and post-injection time as factors for each drug separately. Effects of each of the drug groups compared to the control group were investigated by post-hoc tests using the Tukey-Kramer method. For a direct comparison with previous studies on ketamine (Gass et al., 2014; Grimm et al., 2015), we regarded a subnetwork consisting of prefrontal and hippocampal regions.

### 4.3.6 Network analysis

First we normalized the connection weights by the individual maximum value and thresholded the connectivity matrices by preserving the strongest edges (20th to 45th percentile, 5% increment). We chose a relatively high minimum density of 20% to maintain sufficient connectedness. At 20% density less than 10% of nodes were disconnected from the rest of the network. 45% was the highest density with no negatively weighted connections included.

For each subject and each density threshold we calculated several graph theoretical properties of the individual networks using the Brain Connectivity Toolbox (Rubinov & Sporns, 2010, 2011): degree, betweenness centrality, local and global efficiencies, characteristic path length, clustering coefficient, and small world index.

The clustering coefficients and path lengths as well as global and local efficiencies were normalized by the according quantities calculated for a null model, a network generated by randomizing topology while preserving degree and strength distributions (Rubinov & Sporns, 2010, 2011).

Since the choice of an individual threshold is arbitrary we calculated the areas under the curve (AUC), i.e. the averages over the range of thresholds.

Focusing our analysis on the changes in the brain networks induced by the drugs, we subtracted the AUC values of the baseline datasets from those of the post-injection data. Thus we obtained two sets of differences, subsequently called  $\Delta$ -values, for each subject (15 min – pre-injection, 30 min – pre-injection). Effects of the drugs on these  $\Delta$ -values were examined by two-way ANOVA (dose and post-injection time points as factors), followed by post-hoc tests using the Tukey-Kramer method.

### 4.3.7 Exposure-response relationships

Directly after the fMRI measurements, a blood sample was taken from each rat by cardiac puncture to determine the actual drug exposure in the plasma. Exposure-response relationships between drug plasma concentrations and  $\Delta$ -values of global network metrics were assessed by pharmacokinetic-pharmacodynamic (PK-PD) modelling (Meibohm & Derendorf, 1997). We fitted an  $E_{max}$ -model to the network metric differences  $\Delta z$  and the concentrations  $c$ :

$$\Delta z = \Delta z_{min} + \frac{\Delta z_{max} - \Delta z_{min}}{1 + 10^{\log(C_{50}) - \log(c)}}$$

## 4.4 Results

### 4.4.1 Hippocampal-prefrontal subnetwork

Results of the post-hoc tests for connectivity in the Hc-PFC subnetwork are shown in Figure 10. For comparison we generated according graphs using the data from our previous ketamine study (Gass et al., 2014). Post-hoc tests were performed for connections showing significant main effects of dose ( $p < 0.05$ ).

Traxoprodil at the high dose strengthened many connections between hippocampal and prefrontal regions. At the low and medium doses connections within the PFC were weakened. Lanicemine caused partly overlapping but fewer significant changes. At the high and low doses intra PFC connectivity was decreased, at the medium dose retrosplenial-hippocampal connectivity was increased. As previously reported, ketamine strengthened hippocampal-prefrontal coupling as well. In contrast to the drugs investigated here, it enhanced intra PFC connectivity.

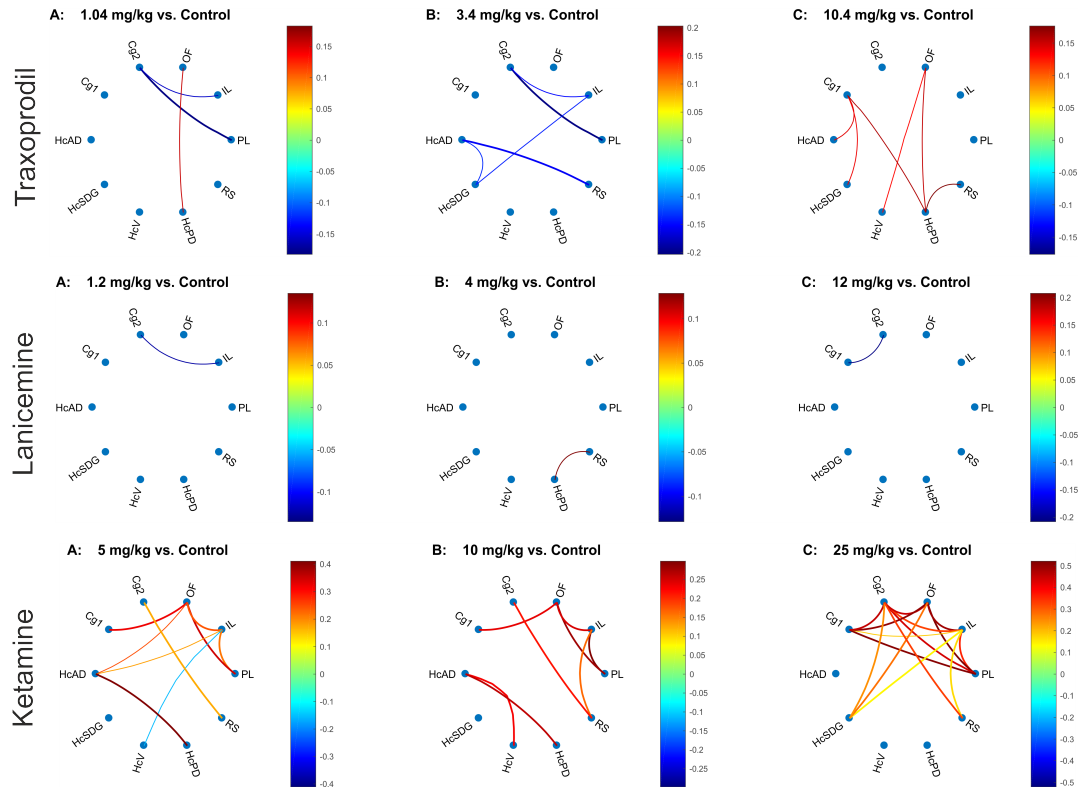


**Figure 10:** Effects on Hc-PFC network: Significant results of post hoc tests (Tukey-Kramer method,  $p < 0.05$ ) between control and each of the dose groups. Colors represent mean group differences of  $\Delta$ -values in Pearson correlation coefficients. Only connections with significant ( $p < 0.05$ ) effect of dose in the ANOVA were considered in the post hoc tests. Thicker lines indicate significance after FDR correction. Ketamine results are shown for comparison and were obtained from the data of our previous study (Gass et al., 2014). (Cg1/2: cingulate cortex, OF: orbitofrontal cortex, IL/PL: infra-/prelimbic cortex, HcAD/SDG/V/PD: Hippocampus (anterior-dorsal/subiculum-dentrate gyrus/ventral/posterior-dorsal), RS: retrosplenial cortex)

#### 4.4.2 Overlapping effects

Despite the strong differences in results between drugs and doses, there were several connections consistently altered by various doses of both drugs (Figure 11) Effects were considered overlapping, if they were significant and in the same direction in at least three of the six comparisons to the control group and in at least one comparison for each substance. Significance for the individual group comparisons is summarized in the table included in Figure 11.

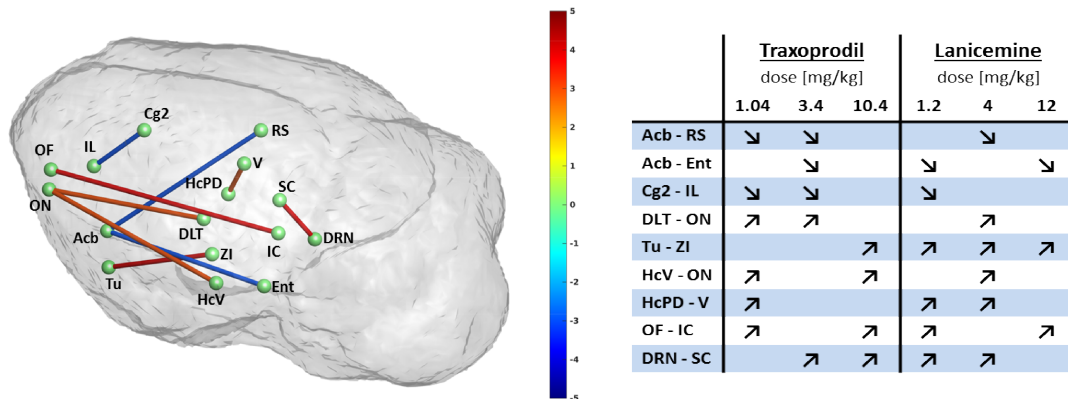


**Figure 11:** Overlapping effects of traxoprodil and lanicemine: Connections are shown if an effect was found in at least half of the groups compared to controls and at least one group for each substance. Colors represent the number of group comparisons showing significant differences with the sign referring to the direction of the effect compared to the control group. The groups contributing to the overlapping effect are indicated in the table on the right.

(OF: orbitofrontal cortex, ON: olfactory nucleus, IL: infralimbic cortex, Cg2: cingulate cortex, Acb: nucleus accumbens, RS: retrosplenial cortex, V: visual cortex, Tu: olfactory tubercle, ZI: zona incerta, HcV/HcPD: ventral/posterior dorsal hippocampus, SC/IC: superior/inferior colliculus, DLT: dorsal lateral thalamus, DRN: dorsal raphe nucleus)

Despite the different patterns of connectivity changes induced by both drugs there were no directly contradicting effects, i.e. connections significantly increased by one but decreased by the other drug.

#### 4.4.3 Network properties

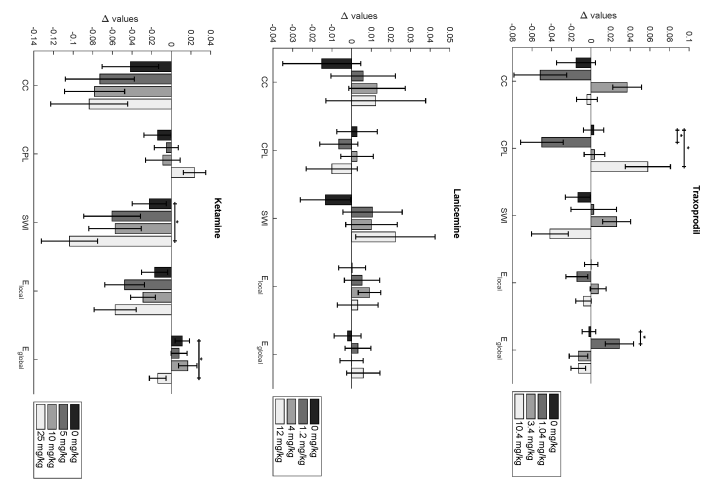
The differences of network properties and the results of the ANOVA and post hoc tests are summarized in Figure 12.

##### Global metrics

The low dose of traxoprodil significantly increased global efficiency and decreased characteristic path length, indicating improved network integration. In contrast, the high dose had the opposite effect.

There was no significant effect of any dose of lanicemine on any of the global network metrics. Despite the lack of significance, lanicemine did not show fundamentally different effects for different doses.

A



B

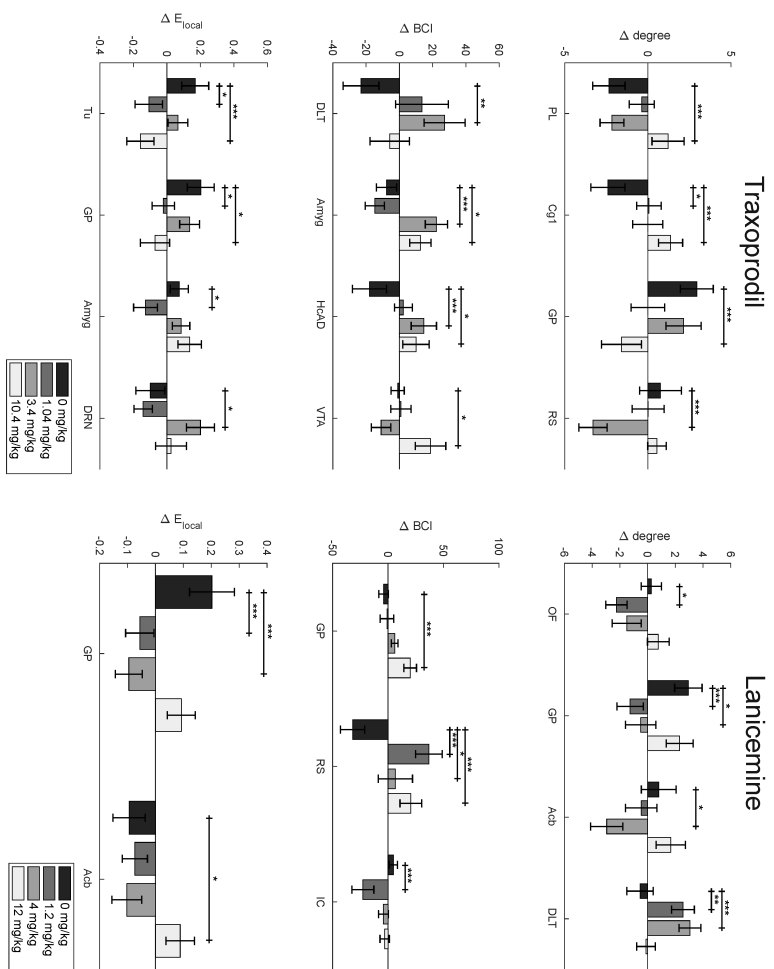


**Figure 12: A:** Average  $\Delta$ -values ( $\pm$  standard error of the mean) of global network properties for dose groups. Significance was tested by a two-way ANOVA and post hoc testing. \* denotes  $p < 0.05$  uncorrected.

(CC: clustering coefficient, CPL: characteristic path length, SWI: small-worldness index,  $E_{global/local}$ : global/average local efficiency)

**B:** Significant differences of drug doses on local network properties. Only regions with significant ( $p < .05$ ) dose effects in the two-way ANOVA are shown. Bars represent group means of delta-values with standard error of the mean as error bars. Horizontal lines indicate significant differences to the control group in post hoc tests. \* denotes  $p < 0.05$  uncorrected, \*\*  $p < 0.05$  Tukey-Kramer pairwise comparison, \*\*\*  $p < 0.05$  Bonferroni-corrected for the number of post-hoc tests.

(BCI: betweenness centrality index,  $E_{local}$ : local efficiency, PL: prelimbic cortex, Cg1: cingulate cortex, GP: globus pallidus, RS: retrosplenial cortex, DLT: dorsolateral thalamus, Amyg: amygdala, HcAD: anterior dorsal hippocampus, VTA: ventral tagmental area, Tu: olfactory tubercle, DRN: dorsal raphe nucleus, OF: orbitofrontal cortex, Acb: nucleus accumbens, IC: inferior colliculus.)



The effect of ketamine on global graph metrics clearly increased with the dose. For the high dose we found a loss of efficiency and small-worldness indicating decreased network integration.

None of the drugs had significant effects of post-injection time.

### Local metrics

There were significant differences between the drug groups and the control group for local network properties of several regions. Again the results for the different doses of traxoprodil were clearly different without directly contradicting each other. The medium dose induced a decrease in the degree of the retrosplenium, whereas it increased the betweenness centrality index (BCI) of dorsolateral thalamus (DLT), amygdala, and anterior dorsal (HcAD). It also increased the local efficiency of the dorsal raphe nucleus (DRN). The effects of the high and low doses were very different from those of the medium dose, while being relatively similar to each other, e.g. increased degree of the cingulate cortex (Cg1), decreased local efficiency of olfactory tubercle (Tu) and globus pallidus. Similar to the medium dose, the high one increased BCI in the amygdala and HcAD. In contrast, the low dose reduced the efficiency of the amygdala.

Lanicemine exhibited more consistent effects across doses. BCI of the retrosplenium was increased by all doses. The medium dose also reduced degree and local efficiency of globus pallidus as well as degree of nucleus accumbens and increased the degree of DLT. The effects of the low dose were generally in line with those of the medium dose, whereas the high dose showed an increase in local efficiency of nucleus accumbens and BCI of globus pallidus.

The globus pallidus was the only region where a direct overlap of the results for both drugs could be found.

#### 4.4.4 PK-PD-models

Fitting of PK/PD models was successful for most network metrics in both groups. Figure 13 shows  $\Delta z$ -log(c) plots for traxoprodil and lanicemine. Consistent with the dose-based analyses described above, exposure response relationships were more pronounced in the traxoprodil than the lanicemine group and there was no difference between measurement timepoints (according figure for 15 min measurement in supplementary material, Figure 15). The  $E_{max}$  model fits indicate increased characteristic path length and decreased global efficiency in response to traxoprodil. Exposure to lanicemine caused an increase in characteristic path length and a decrease in small-worldness.

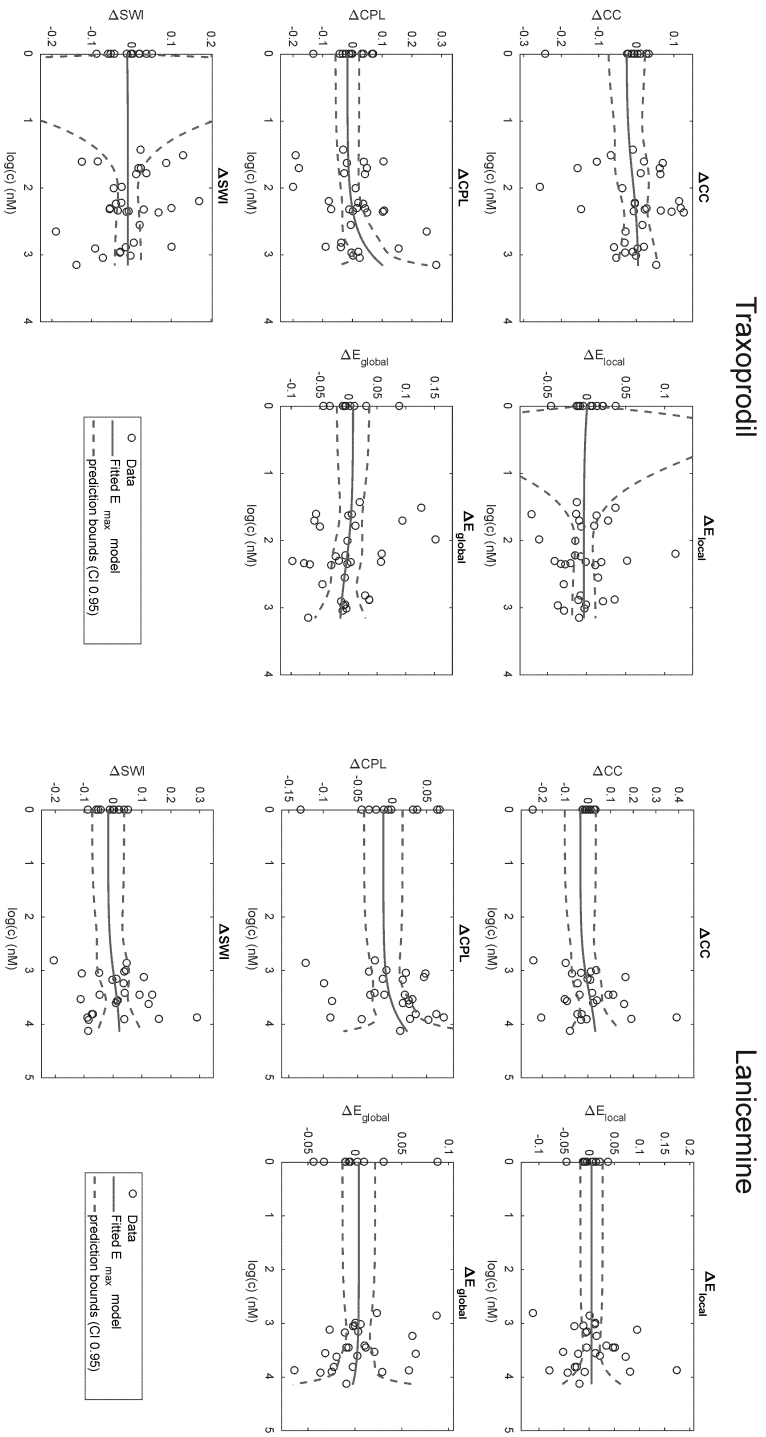


**Figure 13:**  $\Delta$  network metrics (30 min - baseline) vs plasma concentration of traxoprodil (left) and lanicemine (right) respectively. Solid lines show the  $E_{max}$  model fitted to the data, dashed lines show prediction bounds of the fits with confidence interval 0.95. **Traxoprodil:**  $E_{max}$  model fits reveals increase in characteristic path length and decrease in global efficiency. In the low dose group there are three subjects showing considerably higher efficiency and lower characteristic path length. **Lanicemine:**  $E_{max}$  model fits reveals increase in small-worldness and decrease in characteristic path length. (CC: clustering coefficient, CPL: characteristic path length, SWI: small-worldness index, Eglobal/local: global/average local efficiency)

## 4.5 Discussion

### 4.5.1 Hippocampal – prefrontal connectivity

We expected traxoprodil and lanicemine to affect connectivity in the Hc-PFC subnetwork. Hc-PFC coupling is supposed to be critically involved in a variety of psychiatric disorders including depression (Godsil, Kiss, Spedding, & Jay, 2013; Sampath, Sathyanesan, & Newton, 2017). The similarity of findings for traxoprodil and ketamine might reflect the antidepressant effect shared by both drugs. Lanicemine did not affect Hc-PFC coupling, which possibly reflects its limited clinical efficacy.

Connectivity within the PFC was decreased by traxoprodil in contrast to what was found for ketamine. Lanicemine also decreased intra PFC connections, but to a smaller extent than traxoprodil. Decreased intra-prefrontal connectivity is observed in unmedicated depressed patients (Geng et al., 2016; Scheinost et al., 2018). The absence of intra-PFC hyperconnectivity in response to traxoprodil and lanicemine can explain the lack of dissociative side effects, but it might also explain lower antidepressant efficacy. It is highly probable, that dissociative effects are part of the same neurocircuitry as antidepressant effects and both cross in the PFC (Luckenbaugh et al., 2014).

### 4.5.2 Overlapping effects

The decrease of intra PFC connectivity induced by both drugs in contrast to ketamine, is reflected in an overlapping decrease of connectivity between the cingulate cortex (Cg2) and the medial PFC (IL). Most of the parallel effects of both drugs were related to reward circuitry. Connectivity between the nucleus accumbens (Acb), a hub of the reward system and retrosplenial cortex (RS), the homologue of human precuneus/posterior cingulate cortex in the rat, was found to correlate with severity of depression (L. Gong et al., 2017) and speculated to reflect a compensation for impaired reward processing (Hwang et al., 2016). Our observation of reduced FC between these two regions might reflect a pro-hedonic effect of these drugs.

The inferior colliculus (IC) belongs to the brain aversion system, where it gates acoustic information and filters sounds that require immediate action integrating information of aversive nature (de Oliveira, Colombo, Muthuraju, Almada, & Brandao, 2014). Increased connectivity between IC and orbitofrontal cortex (OF), a region implicated in the learning of stimulus-outcome relation-

ship and cognitive flexibility, might improve cognitive control of defensive escapist and fearful reactions and the deficient cognitive flexibility characteristic for depression.

The superior colliculus (SC), in addition to its direct involvement in visual function, also belongs to the brain aversion system. The visually responsive cells in SC are modulated by reward learning (Vuilleumier, 2015) and SC receives projections from the dorsal raphe nucleus (DRN), suggesting that DRN exerts a coordinating influence on the visual system (Villar, Vitale, Hokfelt, & Verhofstad, 1988). Also glutamatergic neurotransmission in the DRN regulates serotonin transmission (Soiza-Reilly & Commons, 2011). Thus, increased connectivity between DRN and SC could improve an affective influence on visual orientation and perception through serotonergic neurotransmission, deficient in depression.

Both drugs elevated connectivity between olfactory tubercle (Tu) and zona incerta (ZI). Tu is part of the ventrostriatal reward system and its stimulation directly promotes reward (Fitzgerald, Richardson, & Wesson, 2014). ZI is involved in limbic-motor integration and deep brain stimulation near or in the ZI alleviates anxiety and depression (Burrows et al., 2012). Therefore, an upregulation of the connectivity between Tu and ZI might improve reward behaviour and reward-related motor control.

Increased connectivity of the olfactory nucleus (ON) might indicate a network phenotype less prone to depression, as olfactory function is suggested to be a marker for vulnerability to depression (Croy & Hummel, 2017).

### 4.5.3 Global network metrics

Our findings suggest an improvement of network integration by traxoprodil at the low dose, but the opposite effect at the high dose. The individual  $\Delta\text{CPL}$  and  $\Delta E_{\text{local}}$ -values show, that the significance of results for the low dose are mainly driven by three subjects in the low dose group (Figure 13). The PK/PD-model fits show trends towards lower network efficiency and longer paths with increasing dose, reflecting a less efficient organization of the network (Figure 13), corresponding well with our previous findings (Gass et al., 2018). In a translational study comparing the effects of ketamine on human and rat brain networks we found small-worldness and global efficiency to be reduced by ketamine in both species (Becker et al., 2016).

For lanicemine no significant group effect was detected for any dose. Nevertheless, small-worldness, global efficiency and clustering tended to increase with dose. These tendencies were also supported by the PK/PD-model fits (Figure 13), although the trends were more subtle than for traxoprodil. The effect of

lanicemine on general network structure tended to be opposite to the effect of traxoprodil, but due to the lack of significance, this tendency cannot be claimed with certainty.

#### 4.5.4 Local network metrics

Similarly to the connectivity and global network results, the effects differed between the doses of traxoprodil. For the medium dose we observed a less central role of RS, which might indicate a downregulation of the default-mode network, which was found to be over-activated in depressed patients (Gudayol-Ferré, Peró-Cebollero, González-Garrido, & Guàrdia-Olmos, 2015; Posner et al., 2015). Its loss of centrality might be an effect of traxoprodil's antidepressant action. Several regions involved in reward processing (amygdala and ventral tagmental area) gained centrality, which again shows the positive effect on reward circuitry assumed to underlie our connectivity results. The less localized role of the olfactory tubercle induced by the high and low doses further supports this interpretation. The DRN was more involved in localized processing, which could also indicate improved reward processing as glutamatergic drive of the DRN regulates serotonergic activity (Soiza-Reilly & Commons, 2011). For the high dose prefrontal and cingulate cortices showed increased centrality due to the strengthened connections to the hippocampus.

In contrast to traxoprodil, lanicemine increased centrality of the RS at all doses. As the RS is a central region of the default mode network (DMN), this effect is opposite to what was expected as a result of antidepressant action. Centrality of the inferior colliculus was significantly decreased by the low dose. Activation of the IC induces defensive behavior and inhibition of glutamatergic receptors in the IC has an anxiolytic effect (de Oliveira et al., 2014). Thus the decreased centrality of IC might indicate a less anxious network phenotype.

One result overlapping between both drugs was a decrease in degree of the globus pallidus. The globus pallidus receives signals from the reward system processing expected reward (Hikosaka, Bromberg-Martin, Hong, & Matsumoto, 2008). Our result might signify an effect on the network mediating reward expectation which could be part of the antidepressant effect, as depression can be triggered by the omission or termination of a reward. (Rolls, 2016).

### 4.5.5 Relation to clinical results

Traxoprodil has been shown to share ketamine's antidepressant effect along with less severe side effects (Preskorn et al., 2008). In general the effects of traxoprodil were not as strong as those of ketamine we found in previous studies, which might be related to the lower efficacy found in clinical studies.

The overlap of clinical effects might be reflected in our results by similar effects on network topology, which are likely to be caused by overlapping changes in connectivity of the hippocampal and prefrontal regions. In MDD patients increased efficiency is explained by a more random structure of the whole brain network (Q. Gong & He, 2015; Zhang et al., 2011). Reduced characteristic path length was found in drug-naïve first-episode MDD (Zhang et al., 2011). Lanicemine shows only short-lived antidepressant action in clinical trials (Sanacora et al., 2014; Zarate et al., 2013). Our results reflect these findings by the lack of significant effects on network topology and Hc-PFC coupling. The extent to which the drugs improve prefrontal-hippocampal coupling correspond well to the clinical results. Thus, improved coupling appears to be strongly associated with the antidepressant effect.

Regarding dissociative side effects, both traxoprodil and lanicemine show more favourable profiles than ketamine, which induces various dissociative effects in up to 50% of subjects (Vollenweider & Kometer, 2010) and even 76% of MDD patients (Zarate et al., 2006). Such effects were rarely observed for traxoprodil (Preskorn et al., 2008) and not reported for lanicemine (Zarate et al., 2013). As this corresponds well to the effect on intra-PFC connectivity, we conclude that effects on the connectivity within the PFC might rather reflect the dissociative effects of NMDA antagonists than their antidepressant effects, although there is evidence for a correlation of both effects (Luckenbaugh et al., 2014).

The effects overlapping between the drugs, i.e. overlapping connectivity changes and regional network alterations, were related to improved reward processing. As many aspects of reward processing were found to be impaired in depression, these network improvements might contribute to the clinical results.

### 4.5.6 Limitations

One possible confounding effect might be drug-anesthesia interactions. Medetomidine sedation is preferred over other anesthetic protocols due to its small effect on neuronal activity (Nasrallah, Tan, & Chuang, 2012). Moreover, functional connectivity in medetomidine sedated rats is similar to humans (Williams et al., 2010). In translational studies comparing the effects of ketamine on hu-

mans and sedated rats, we found no signs of anesthetic effects despite high doses of the drug (Becker et al., 2016; Grimm et al., 2015). Thus, the sedation we applied appears to be sufficiently light to avoid interaction effects.

This study was designed to investigate the acute effects of NMDA antagonists. Clinical studies of the same drugs found effects on a timescale of hours to days which was not covered by our investigation.

## 4.6 Conclusion

In general traxoprodil induced greater differences in brain networks than lanicemine, while neither of the two reached the level of the ketamine effects. The action on the hippocampal-prefrontal network corresponded well to the antidepressant efficacy found in clinical studies. Thus, hippocampal-prefrontal coupling as well as connectivity within the PFC are possible targets for further investigation. Especially, the relationship of hippocampal-prefrontal connectivity and antidepressant effects could yield further insight to the action of NMDA receptor antagonists and their possible application in therapy of depression. The effects for both drugs differed across doses, partly even opposing trends were observed. Nevertheless there were consistent findings across doses and drugs. Most of the effects we found for both traxoprodil and lanicemine reflect improvement of reward processing which might underlie the clinical effects. Further investigation of the effects of NMDA antagonists on the reward system might yield more insight into the neurobiological mechanisms underlying depression and antidepressant treatment. Translational studies might be helpful to identify promising compounds early within the drug discovery process.

## 4.7 Supplementary material

### 4.7.1 Methods

#### ICA denoising

In order to get rid of nuisance signals in our fMRI data we applied a denoising approach based on independent component analysis (ICA). The basic idea is to decompose the 4D fMRI images, i.e. voxelwise timeseries, into a number of independent components, then identifying the components representing noise and remove them before reconstructing the images from the remaining good components. As suggested by Hyvärinen et al. (Hyvärinen et al., 2001), we ran a principal component analysis (PCA) as preliminary step, in order to

determine the optimal number of components, which we found to be between 10 and 15. Thus, we decomposed the data into 12 components. Examples of average image timecourses and component timecourses are shown in Figure 14.

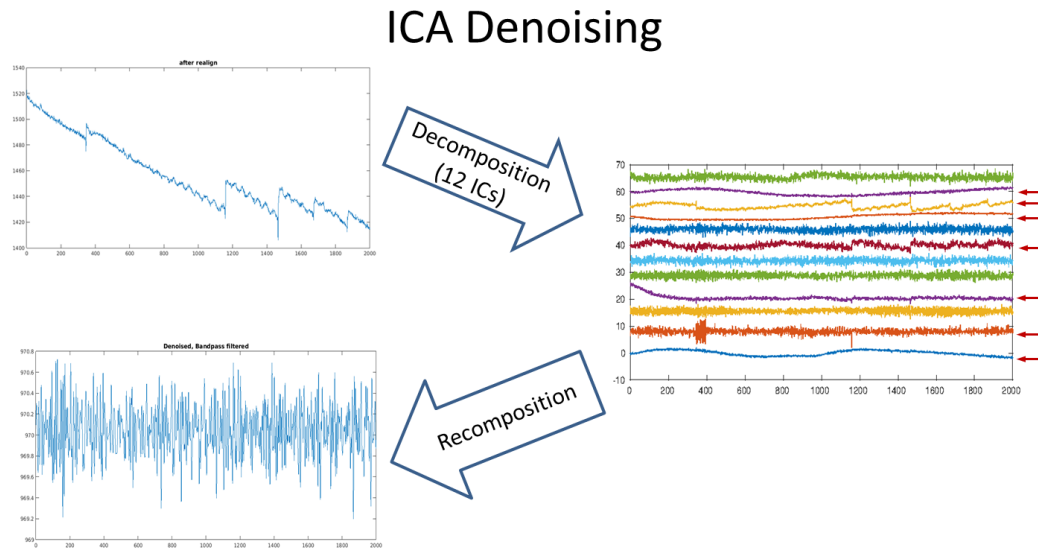


**Figure 14:** ICA Denoising procedure: Decomposition of fMRI signal into 12 independent components (IC), exclusion of components if timecourses (or derivatives) correlate ( $R > 0.2$ ) with realignment parameters/CSF signal or have large spikes (marked with red arrows).

The crucial point in this denoising procedure is the identification of components reflecting undesired nuisance signals. Mostly researchers using ICA methods for denoising classify components as signal or noise by visual inspection (Kelly et al., 2010). We chose an automated procedure avoiding the subjective nature of manual classification. The routine we implemented was inspired by the ICA-AROMA tool (Pruim et al., 2015), however we used a simplified approach. The classification was based on the component timecourses regardless of spectral content or spatial distribution of the components. Components were excluded if their timecourses correlated ( $R > 0.2$ ) with any of the realignment parameters or the average timecourse from the CSF or any of their derivatives. Additionally components were considered to reflect artefactual signal if peaks occurring in their timecourses exceeded 5 standard deviations in height. The same criteria were applied to the temporal derivatives of the timecourses.



## Graph metrics

First we normalized the remaining connection weights by the individual maximum value and thresholded the connectivity matrices by preserving the strongest edges (20th to 45th percentile, 5% increment). We chose a relatively high minimum density of 20% to maintain a sufficient degree of connectedness of the network. At 20% density less than 10% of nodes were disconnected from the rest of the network. 45% was the highest density with no negatively weighted connections included and therefore the logical choice for maximum density.

For each subject and each density threshold we calculated several graph theoretical properties of the individual networks using the Brain Connectivity Toolbox (Rubinov & Sporns, 2010, 2011):

**Node degree:** The number of connections a node has

**Betweenness centrality:** The fraction of all shortest paths in the network passing through a given node

**Local clustering coefficient:** The fraction of possible connections among the neighbours of a given node weighted by the connection weights

**Global clustering coefficient:** The average of local clustering coefficients across all nodes

**Characteristic path length:** The average weighted length of shortest paths between all pairs of nodes

**Small-world index:** The quotient of clustering coefficient and characteristic path length

**Global efficiency:** Average inverse shortest path length

**Local efficiency:** Efficiency of the neighbourhood of a given node

The clustering coefficients and path lengths as well as global and local efficiencies were normalized by the according quantities calculated for a null model, a network generated by randomizing topology while preserving degree and strength distributions (Rubinov & Sporns, 2010, 2011).

## 4.7.2 Additional results

### PK/PD-modelling

$E_{max}$ -fits of the network metrics 30 min after injection did not principally differ from those of the 15 min networks, which are shown in Figure 15. The similarity between the 15 min and 30 min plots reflects the absence of significant effects of time in the 2-way-ANOVAs of graph metrics.

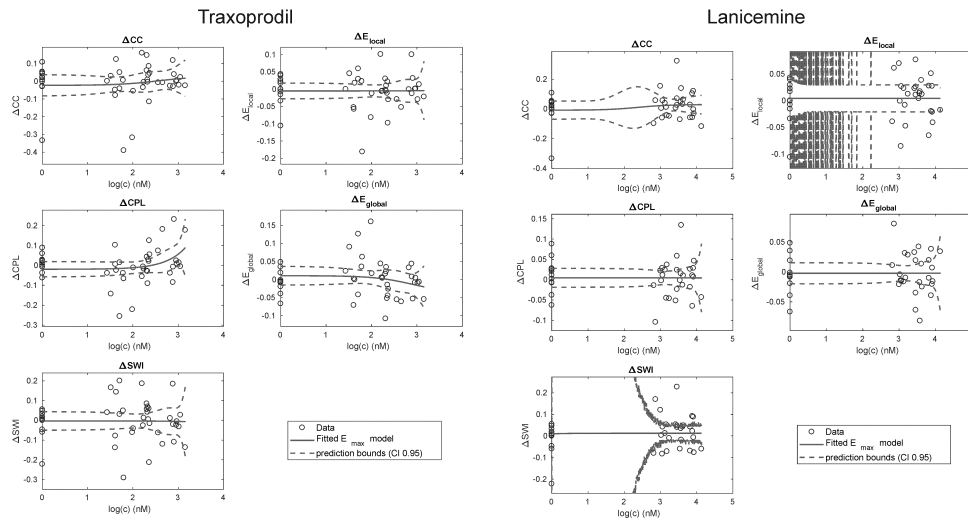


**Figure 15:**  $\Delta$  network metrics (15 min - baseline) vs concentration of traxoprodil in the brain.  $E_{max}$  model fits reveals increase in characteristic path length and decrease in global efficiency. In the low dose group there are three subjects showing considerably higher efficiency and lower characteristic path length.

# 5

## Discussion

### 5.1 Establishment of network methods in preclinical studies

One aim of this work was to translate network methods, which are well established in clinical studies, to the realm of preclinical research in rats. The translatability of results to clinical investigations is an important issue in preclinical research. Despite the translational potential of network methods, studies directly comparing brain networks across species are rare.

In the translational study presented in chapter 3, ketamine induced largely congruent network reconfigurations in humans and rats. In both species ketamine reduced network integration while increasing segregation. The effect of ketamine on interregional connectivity was also comparable in humans and rats. Prefrontal connectivity was increased in both species. With this study directly comparing results in humans and rats, network scientific methods have been shown to provide results which are translatable across species. With this direct translational approach, we demonstrated that properties of brain networks can be valuable biomarkers for translational drug research.

In addition to the studies presented in detail in chapters 3 and 4, similar network methods have been applied in another pharmacological study investigating effects of NMDA antagonists. Gass et al. (2018) found network alterations induced by ketamine and traxoprodil which were comparable to what is presented above, which further supports the validity and reliability of network methods.

Furthermore, the usage of the network methods, which were implemented in the course of this project, is not restricted to pharmacological studies. The methods have been used for several studies conducted by the research group Translational Imaging in recent years (see 2.3). We found network effects in animal models of depression (Gass et al., 2016; Clemm von Hohenberg et al., 2018), early life stress (Reinwald et al., 2018) and neuropathic pain (Bilbao et al., 2018). The variety of studies on different subjects of research, in which we found network alterations, demonstrates the methods' versatility for all kinds of rs-fMRI studies and shows that they have been established as part of the resting state analysis routine.

## 5.2 Effects of NMDA antagonists on rat brain networks

The network effects of three NMDA antagonists (ketamine, traxoprodil, and lanicemine) were investigated in order to find potential relationships of functional networks with the antidepressant effect of these drugs. In the study presented in chapter 4 network effects of traxoprodil and lanicemine have been investigated and compared to each other and to the effects of ketamine. Comparing the effects of antagonists differing in their mechanisms of action, might help gaining insight into the relationship of biochemical mechanisms, network effects, and clinical efficacy.

While ketamine greatly increased hippocampal-prefrontal coupling in an earlier study (Gass et al., 2014), the increase caused by traxoprodil was weaker and lanicemine hardly induced any significant changes. Hippocampal-prefrontal pathways are involved in a variety of fundamental cognitive processes (e.g. working memory and learning) and are impaired by various psychiatric disorders including depression (Godsil et al., 2013; Sampath et al., 2017). Furthermore the Hc-PFC network and its response to ketamine have been found across species (Schwarz, Gass, Sartorius, Zheng, et al., 2013; Grimm et al., 2015). Considering the results of clinical studies, showing stronger antidepressant action for ketamine than for traxoprodil and only short lived effect of lanicemine

(Zarate et al., 2006; Preskorn et al., 2008; Zarate et al., 2013), our results support the hypothesis that hippocampal-prefrontal coupling is a key feature of glutamatergic antidepressants.

Interestingly, the connectivity within the PFC was increased by ketamine but decreased by traxoprodil. Possibly this reflects the more severe dissociative side effects of ketamine. However it also might reflect its higher antidepressant efficacy, as it is suspected that antidepressant and dissociative effects originate from the same or at least overlapping neurocircuitry (Luckenbaugh et al., 2014; Niciu et al., 2018).

Ketamine and traxoprodil evoked a reduction of network integration and small-worldness. Lanicemine had no significant effect on global network properties but the tendencies of the insignificant results suggest improved integration contradicting the results of ketamine and traxoprodil. In MDD patients increased network integration was found and interpreted as more randomized network structure (Q. Gong & He, 2015; Zhang et al., 2011). Ketamine and traxoprodil possibly act antidepressantly by counteracting this randomization. However it has to be noted that network effects of depression are diverse due to the heterogeneity of the disease and large variation of patient cohorts (e.g. medication, age, stage of depression, comorbidities).

Traxoprodil and lanicemine showed overlapping effects on many functional connections involving regions related to the reward system. Among others, connections of the ventral striatum (nucleus accumbens and olfactory tubercle), dorsal raphe nucleus as well as thalamic and hippocampal regions were affected. Regarding graph theoretical metrics, betweenness centrality of reward related regions like hippocampus, amygdala and thalamus were improved by traxoprodil. All these results suggest an improvement of reward processing induced by the drugs. In a very similar study, we found according effects for ketamine and traxoprodil (Gass et al., 2018). Impaired function of the reward system was found in patients suffering from depression (Satterthwaite et al., 2015). Thus, our findings suggest that the antidepressant effect of NMDA antagonists might be mediated by improved reward processing.

All drugs examined here, ketamine, traxoprodil, and lanicemine induced significant network alterations. However, the effects of traxoprodil and lanicemine were less pronounced than those of ketamine. Despite partly parallel results, lanicemine appears to act differently from ketamine and traxoprodil, which is possibly related to its lower efficacy in clinical studies. Traxoprodil's effect on brain networks were largely similar to those of ketamine. As traxoprodil, unlike ketamine, specifically acts on the NR2B subtype of NMDA receptors, these findings support the hypothesis that antidepressant effects of both drugs are driven by the action on that subtype.

## 5.3 Limitations

The effects of ketamine and traxoprodil on brain networks were generally congruent. However there are some methodological limitations to be considered. The network definition strategies differed between the two studies presented in chapters 3 and 4 respectively. In the translational ketamine study we examined binarized networks at relatively low densities between 0.05 and 0.2. The effects of traxoprodil and lanicemine were studied in weighted networks with higher densities between 0.2 and 0.45. Nevertheless, the global network results for ketamine presented in chapter 4 (Figure 12 which were calculated from the same ketamine dataset for comparison, are very similar to those in the translational study. Thus the drug effects appear to be independent of binarization and choice of network density to some extent.

Another aspect possibly confounding the comparability of results is the variance in image preprocessing between the studies. Especially the filtering of motion artefacts differs between linear regression of motion parameters in the ketamine rats and different ICA based methods in the human ketamine group as well as the traxoprodil and lanicemine study. Again, the similarity of results for ketamine and traxoprodil across studies (also in comparison to Gass et al. (2018)) indicates their robustness regardless of the preprocessing strategy.

Finally, the studies discussed here all focussed on the acute effects of the drugs. There is evidence however that the antidepressant effect of the drugs is different on the timescale of hours or days.

## 5.4 Future work

To better understand the action of NMDA antagonists and more importantly to evaluate their antidepressant potential, it is important to relate the network findings more closely to depression. In order to achieve this rapprochement to depression, functional connectivity data from a study using ketamine treatment in a rat model of depression is already being analysed.

Recently, there is growing interest in dynamic brain connectivity in the neuroscience community, since the resting state was found to be less stable than expected (Chang & Glover, 2010; Bassett et al., 2013). Figure 16 shows the principle of dynamic network analysis using a sliding window approach. Networks are calculated in the same way as with static connectivity, but only over a small time window (usually a few minutes) of the regional fMRI signals. By sliding the window over the total length of the timecourses, a series of networks is calculated. Thus, the dynamics of network behaviour can be analysed.

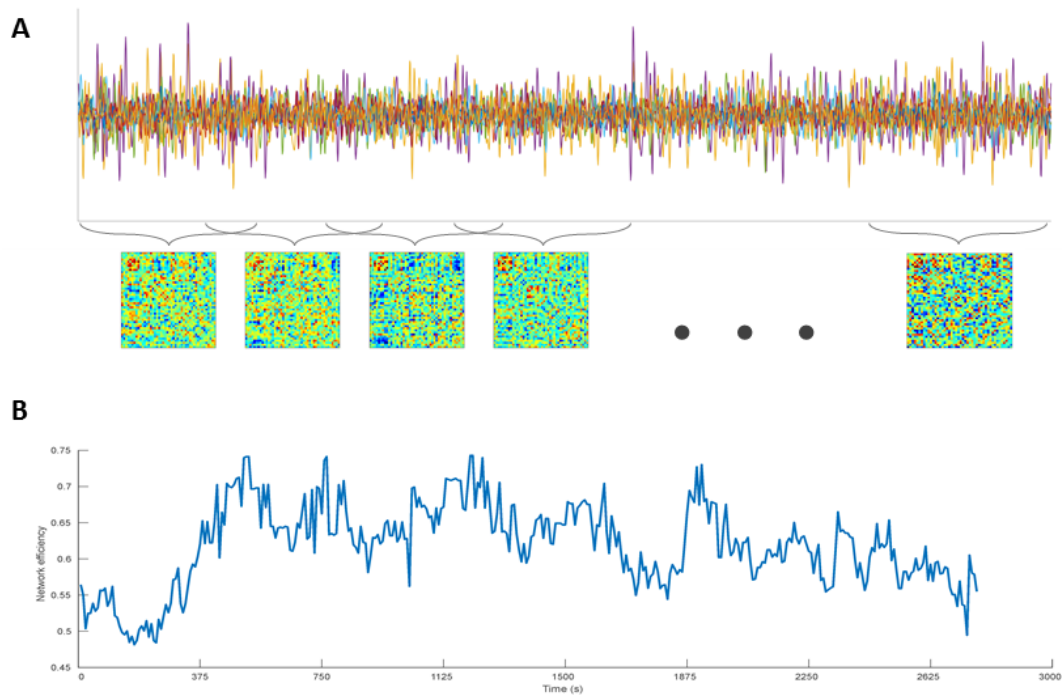


**Figure 16:** *Dynamic network analysis. A: A series of networks is calculated according to the static case by sliding the time window of interest over the total length of the timecourses. B: Dynamics of network efficiency for a single subject*

Figure 16 shows data of a single traxoprodil treated subject from the study presented in chapter 4. The variation visible in both, network matrices(A) and network efficiency(B) show that network dynamics are a promising subject of future research.

Making use of these methods could be especially interesting for pharmacological network studies, as they might facilitate time-resolved measurement of acute drug effects. The acute and long term effects of NMDA antagonists are supposed to differ. Thus, observing the effects of the drug with higher temporal resolution might yield further insight into their mechanisms of action.

## 5.5 Conclusion

### **Network methods provide reliable results across studies and species**

In the course of this work, network scientific methods using the formalism of graph theory were successfully implemented. The translational validity of these methods in pharmacological studies was shown in a study directly comparing network effects of ketamine between humans and rats. Furthermore, network methods were established as part of the resting state analysis routine and applied in various studies.

### **Congruent effects of ketamine and traxoprodil suggest important role of NR2B subtype**

The effects of traxoprodil, increased hippocampal-prefrontal coupling and reduced network integration, were congruent with effects of ketamine. Since traxoprodil specifically acts on the NR2B subtype of the receptor, these findings support the hypothesis, that NR2B receptors are especially involved in the antidepressant action of the drugs.

### **Contradicting effects on intra-PFC coupling possibly related to dissociative effect**

Unlike ketamine, traxoprodil and lanicemine did not increase intra-PFC connectivity. This contradiction in the network effects might be related to the more severe dissociative effects reported for ketamine.

### **Acute antidepressant effect possibly mediated by improved reward processing**

All three drugs induced an improvement of reward processing represented in local network properties as well as overlapping connectivity effects. Thus the overlapping acute but short lived antidepressant effect might be mediated by improved reward processing.



# Summary

In recent years network methods have gained great popularity in the analysis of resting state data obtained by functional magnetic resonance imaging (fMRI). Network alterations have been found to be induced by various psychiatric disorders as well as drug induced states. Depression, being one of the most prevalent psychiatric disorders, is of special interest for psychiatric research. Brain networks have been found to be affected by depression in many clinical studies examining a variety of patient cohorts (different ages, types of depression, treatment status).

Ketamine, an N-methyl-d-aspartate (NMDA) receptor antagonist, was found to act antidepressantly at sub anaesthetic doses. In contrast to conventional antidepressants (e.g. selective serotonin reuptake inhibitors), ketamine acts very quickly (within hours) and reliably even in treatment resistant patients. However ketamine also induces dissociative effects, often perceived as aversive. Since this discovery was made, other NMDA receptor antagonists are examined as potential glutamatergic antidepressants sharing ketamine's antidepressant action but not its dissociative effects. Two candidate drugs were investigated here: Lanicemine (AZD7665), a low trapping NMDA channel blocker, and traxoprodil, a non-competitive antagonist targeting the NR2B subgroup of the receptor.

One objective of this work was the translation of network methods mostly developed for human studies to preclinical fMRI and the demonstration of their translational potential in a study comparing effects of ketamine across species. Network alterations were supposed to be similar in humans and rats.

As expected, we found largely congruent effects (see chapter 3). In both species ketamine induced a more segregated network structure as well as large-scale connectivity alterations. These results show the direct translatability of network methods across species and therefore underline their potential for pre-clinical neuroscientific research.

Furthermore the network effects of traxoprodil and lanicemine were investigated in another fMRI study in rats (see chapter 4). Based on to the effects of ketamine found in previous studies we expected increased connectivity in the hippocampal-prefrontal (Hc-PFC) network as well as reduced network integration. For traxoprodil results were expected to be generally similar to those found

for ketamine. Due to its similar mechanism of action we expected similar but less pronounced results for lanicemine compared to ketamine. Nevertheless, deviating results between different NMDA antagonists might help explaining the mechanisms underlying their effects.

Like ketamine, traxoprodil induced an increase in Hc-PFC coupling, however its effect was less pronounced. Lanicemine hardly had any significant effect on this subnetwork. The extent to which Hc-PFC coupling was induced by the three drugs corresponds well to their antidepressant efficacy in clinical trials, which suggests a central role of Hc-PFC coupling in the action of glutamatergic antidepressants.

Regarding the effects on graph theoretical network properties, traxoprodil and ketamine induced a reduction of network integration. Once more, the effects induced by ketamine and traxoprodil were similar, while lanicemine had no significant effect. This again reflects the clinical efficacy of the drugs.

All three drugs induced improvement of reward processing as reflected by connectivity alterations and effects on local network properties in reward related brain areas.

The differing results for Hc-PFC coupling and global network properties suggest that lanicemine's lower clinical efficacy compared to ketamine and traxoprodil is related to these network phenotypes.

Since traxoprodil exclusively acts on the NR2B subtype of the NMDA receptor, the parallel results suggest a central role of this subtype for the action of glutamatergic antidepressants.

Acute and long-term effects of NMDA antagonists are supposed to differ considerably. Thus, the dynamics of network effects deserves further research. Data comparing acute and long-term effects of ketamine on functional networks are already being analysed. Future investigations of network dynamics could benefit from recent advances in dynamic connectivity methodology.

# Bibliography

- Achard, S., Salvador, R., Whitcher, B., Suckling, J., & Bullmore, E. (2006). A resilient, low-frequency, small-world human brain functional network with highly connected association cortical hubs. *Journal of Neuroscience*, *26*(1), 63–72. doi:10.1523/JNEUROSCI.3874-05.2006
- Anticevic, A., Corlett, P. R., Cole, M. W., Savic, A., Gancsos, M., Tang, Y., ... Krystal, J. H. (2015). N-methyl-d-aspartate receptor antagonist effects on prefrontal cortical connectivity better model early than chronic schizophrenia. *Biological Psychiatry*, *77*(6), 569–580. doi:10.1016/j.biopsych.2014.07.022
- Artigas, F., Schenker, E., Celada, P., Spedding, M., Llado-Pelfort, L., Jurado, N., ... Schwarz, A. J. (2017). Defining the brain circuits involved in psychiatric disorders: IMI-NEWMEDS. *Nat Rev Drug Discov*, *16*(1), 1–2. doi:10.1038/nrd.2016.205
- Autry, A. E., Adachi, M., Nosyreva, E., Na, E. S., Los, M. F., Cheng, P.-f., ... Monteggia, L. M. (2011). NMDA receptor blockade at rest triggers rapid behavioural antidepressant responses. *Nature*, *475*, 91. doi:10.1038/nature10130
- Bähner, F., Demanuele, C., Schweiger, J., Gerchen, M. F., Zamoscik, V., Ueltzhöffer, K., ... Meyer-Lindenberg, A. (2015). Hippocampal-dorsolateral prefrontal coupling as a species-conserved cognitive mechanism: A human translational imaging study. *Neuropsychopharmacology*, *40*, 1674. doi:10.1038/npp.2015.13
- Bassett, D. S. & Bullmore, E. (2006). Small-world brain networks. *Neuroscientist*, *12*(6), 512–523. doi:10.1177/1073858406293182
- Bassett, D. S., Bullmore, E., Verchinski, B. A., Mattay, V. S., Weinberger, D. R., & Meyer-Lindenberg, A. (2008). Hierarchical organization of human cortical networks in health and schizophrenia. *J Neurosci*, *28*(37), 9239–48. doi:10.1523/JNEUROSCI.1929-08.2008

- Bassett, D. S., Greenfield, D. L., Meyer-Lindenberg, A., Weinberger, D. R., Moore, S. W., & Bullmore, E. T. (2010). Efficient physical embedding of topologically complex information processing networks in brains and computer circuits. *PLOS Computational Biology*, *6*(4), e1000748. doi:10.1371/journal.pcbi.1000748
- Bassett, D. S., Nelson, B. G., Mueller, B. A., Camchong, J., & Lim, K. O. (2012). Altered resting state complexity in schizophrenia. *NeuroImage*, *59*(3), 2196–2207.
- Bassett, D. S., Porter, M. A., Wymbs, N. F., Grafton, S. T., Carlson, J. M., & Mucha, P. J. (2013). Robust detection of dynamic community structure in networks. *Chaos*, *23*(1), 013142. doi:10.1063/1.4790830
- Bassett, D. S. & Sporns, O. (2017). Network neuroscience. *Nature Neuroscience*, *20*, 353. doi:10.1038/nn.4502
- Becerra, L., Upadhyay, J., Chang, P. C., Bishop, J., Anderson, J., Baumgartner, R., . . . Borsook, D. (2013). Parallel buprenorphine phMRI responses in conscious rodents and healthy human subjects. *Journal of Pharmacology and Experimental Therapeutics*, *345*(1), 41–51. doi:10.1124/jpet.112.201145
- Becker, R., Braun, U., Schwarz, A. J., Gass, N., Schweiger, J. I., Weber-Fahr, W., . . . Meyer-Lindenberg, A. (2016). Species-conserved reconfigurations of brain network topology induced by ketamine. *Transl Psychiatry*, *6*, e786. doi:10.1038/tp.2016.53
- Becker, R., Gass, N., Kußmaul, L., Schmid, B., Scheuerer, S., Schnell, D., . . . Sartorius, A. (Submitted). NMDA receptor antagonists traxoprodil and lanicemine improve hippocampal-prefrontal coupling and reward related networks in rats. *Neuropsychopharmacology*.
- Berman, R. M., Cappiello, A., Anand, A., Oren, D. A., Heninger, G. R., Charney, D. S., & Krystal, J. H. (2000). Antidepressant effects of ketamine in depressed patients. *Biological Psychiatry*, *47*(4), 351–354. doi:10.1016/S0006-3223(99)00230-9
- Bilbao, A., Falfán-Melgoza, C., Leixner, S., Becker, R., Singaravelu, S. K., Sack, M., . . . Weber-Fahr, W. (2018). Longitudinal structural and functional brain network alterations in a mouse model of neuropathic pain. *Neuroscience*.
- Biswal, B., Zerrin Yetkin, F., Haughton, V. M., & Hyde, J. S. (1995). Functional connectivity in the motor cortex of resting human brain using echo-planar MRI. *Magn. Reson. Med.* *34*(4), 537–541. doi:10.1002/mrm.1910340409

- 
- Blondel, V. D., Guillaume, J.-L., Lambiotte, R., & Lefebvre, E. (2008). Fast unfolding of communities in large networks. *Journal of Statistical Mechanics: Theory and Experiment*, 2008(10), P10008. doi:10.1088/1742-5468/2008/10/p10008
- Braun, U., Muldoon, S. F., & Bassett, D. S. (2015). On human brain networks in health and disease. In *Els* (pp. 1–9). American Cancer Society. doi:10.1002/9780470015902.a0025783
- Braun, U., Plichta, M. M., Esslinger, C., Sauer, C., Haddad, L., Grimm, O., . . . Meyer-Lindenberg, A. (2012). Test-retest reliability of resting-state connectivity network characteristics using fMRI and graph theoretical measures. *Neuroimage*, 59(2), 1404–12. doi:10.1016/j.neuroimage.2011.08.044
- Bressler, S. L. & Seth, A. K. (2011). Wiener-Granger causality: A well established methodology. *NeuroImage*, 58(2), 323–329. doi:10.1016/j.neuroimage.2010.02.059
- Bullmore, E. & Sporns, O. (2009). Complex brain networks: Graph theoretical analysis of structural and functional systems. *Nat Rev Neurosci*, 10(3), 186–98. doi:10.1038/nrn2575
- Burrows, A. M., Ravin, P. D., Novak, P., Peters, M. L., Dessureau, B., Swearer, J., & Pilitsis, J. G. (2012). Limbic and motor function comparison of deep brain stimulation of the zona incerta and subthalamic nucleus. *Neurosurgery*, 70(1 Suppl Operative), 125–30, 125–30. doi:10.1227/NEU.0b013e318232fdac
- Cao, H., Plichta, M. M., Schäfer, A., Haddad, L., Grimm, O., Schneider, M., . . . Tost, H. (2014). Test-retest reliability of fMRI-based graph theoretical properties during working memory, emotion processing, and resting state. *NeuroImage*, 84, 888–900.
- Chai, L. R., Khambhati, A. N., Ciric, R., Moore, T. M., Gur, R. C., Gur, R. E., . . . Bassett, D. S. (2017). Evolution of brain network dynamics in neurodevelopment. *Network Neuroscience*, 1(1), 14–30. doi:10.1162/NETN\_a\_00001
- Chang, C. & Glover, G. H. (2010). Time-frequency dynamics of resting-state brain connectivity measured with fMRI. *Neuroimage*, 50(1), 81–98. doi:10.1016/j.neuroimage.2009.12.011
- Clemm von Hohenberg, C., Weber-Fahr, W., Leibold, P., Ravi, N., Braun, U., Gass, N., . . . Sartorius, A. (2018). Lateral habenula perturbation reduces default-mode network connectivity in a rat model of depression. *Translational Psychiatry*, 8(1), 68. doi:10.1038/s41398-018-0121-y

- Croy, I. & Hummel, T. (2017). Olfaction as a marker for depression. *J Neurol*, *264*(4), 631–638. doi:10.1007/s00415-016-8227-8
- Dawson, N., Xiao, X., McDonald, M., Higham, D. J., Morris, B. J., & Pratt, J. A. (2014). Sustained NMDA receptor hypofunction induces compromised neural systems integration and schizophrenia-like alterations in functional brain networks. *Cerebral Cortex*, *24*(2), 452–464. doi:10.1093/cercor/bhs322
- De Vico Fallani, F., Richiardi, J., Chavez, M., & Achard, S. (2014). Graph analysis of functional brain networks: Practical issues in translational neuroscience. *Philosophical Transactions of the Royal Society of London B: Biological Sciences*, *369*(1653). doi:10.1098/rstb.2013.0521
- de Oliveira, A. R., Colombo, A. C., Muthuraju, S., Almada, R. C., & Brandao, M. L. (2014). Dopamine D2-like receptors modulate unconditioned fear: Role of the inferior colliculus. *PLoS One*, *9*(8), e104228. doi:10.1371/journal.pone.0104228
- Diazgranados, N., Ibrahim, L., Brutsche, N. E., & et al. (2010). A randomized add-on trial of an n-methyl-d-aspartate antagonist in treatment-resistant bipolar depression. *Archives of General Psychiatry*, *67*(8), 793–802. doi:10.1001/archgenpsychiatry.2010.90
- Diestel, R. (2017). *Graph theory* (5th). Springer Publishing Company, Incorporated.
- Doyle, O. M., De Simoni, S., Schwarz, A. J., Brittain, C., O'Daly, O. G., Williams, S. C. R., & Mehta, M. A. (2013). Quantifying the attenuation of the ketamine pharmacological magnetic resonance imaging response in humans: A validation using antipsychotic and glutamatergic agents. *J Pharmacol Exp Ther*, *345*(1), 151.
- Driesen, N. R., McCarthy, G., Bhagwagar, Z., Bloch, M., Calhoun, V., D'Souza, D. C., ... Krystal, J. H. (2013). Relationship of resting brain hyperconnectivity and schizophrenia-like symptoms produced by the NMDA receptor antagonist ketamine in humans. *Mol Psychiatry*, *18*(11), 1199–204. doi:10.1038/mp.2012.194
- Euler, L. (1736). Solutio problematis ad geometriam situs pertinentis. *Comm. Acad. Sci. Imper. Petropol.* *8*, 128–140.
- Fitzgerald, B. J., Richardson, K., & Wesson, D. W. (2014). Olfactory tubercle stimulation alters odor preference behavior and recruits forebrain reward and motivational centers. *Front Behav Neurosci*, *8*, 81. doi:10.3389/fnbeh.2014.00081

- 
- Fornito, A., Zalesky, A., Pantelis, C., & Bullmore, E. T. (2012). Schizophrenia, neuroimaging and connectomics. *Neuroimage*, *62*(4), 2296–314. doi:10.1016/j.neuroimage.2011.12.090
- Furey, M. L., Khanna, A., Hoffman, E. M., & Drevets, W. C. (2010). Scopolamine produces larger antidepressant and antianxiety effects in women than in men. *Neuropsychopharmacology*, *35*, 2479. doi:10.1038/npp.2010.131
- Gargouri, F., Kallel, F., Delphine, S., Ben Hamida, A., Lehericy, S., & Valabregue, R. (2018). The influence of preprocessing steps on graph theory measures derived from resting state fMRI. *Frontiers in Computational Neuroscience*, *12*, 8. doi:10.3389/fncom.2018.00008
- Gass, N., Becker, R., Sack, M., Schwarz, A. J., Reinwald, J. R., Cosa-Linan, A., ... Sartorius, A. (2018). Antagonism at the NR2B subunit of NMDA receptors induces increased connectivity of the prefrontal and subcortical regions regulating reward behavior. *Psychopharmacology*, *235*(4), 1055–1068. doi:10.1007/s00213-017-4823-2
- Gass, N., Becker, R., Schwarz, A. J., Weber-Fahr, W., Clemm von Hohenberg, C., Vollmayr, B., & Sartorius, A. (2016). Brain network reorganization differs in response to stress in rats genetically predisposed to depression and stress-resilient rats. *Translational Psychiatry*, *6*(12), e970. doi:10.1038/tp.2016.233
- Gass, N., Schwarz, A. J., Sartorius, A., Schenker, E., Risterucci, C., Spedding, M., ... Weber-Fahr, W. (2014). Sub-anesthetic ketamine modulates intrinsic bold connectivity within the hippocampal-prefrontal circuit in the rat. *Neuropsychopharmacology*, *39*(4), 895–906. doi:10.1038/npp.2013.290
- Geng, H., Wu, F., Kong, L., Tang, Y., Zhou, Q., Chang, M., ... Wang, F. (2016). Disrupted structural and functional connectivity in prefrontal-hippocampus circuitry in first-episode medication-naive adolescent depression. *PLoS One*, *11*(2), e0148345. doi:10.1371/journal.pone.0148345
- Glover, G. H., Li, T. Q., & Ress, D. (2000). Image-based method for retrospective correction of physiological motion effects in fMRI: RETROICOR. *Magn. Reson. Med.* *44*(1), 162–167. doi:10.1002/1522-2594(200007)44:1<162::aid-mrm23>3.0.co;2-e
- Godsil, B. P., Kiss, J. P., Spedding, M., & Jay, T. M. (2013). The hippocampal-prefrontal pathway: The weak link in psychiatric disorders? *Eur Neuropsychopharmacol*, *23*(10), 1165–81. doi:10.1016/j.euroneuro.2012.10.018

- Gong, L., Yin, Y., He, C., Ye, Q., Bai, F., Yuan, Y., ... Zhang, Z. (2017). Disrupted reward circuits is associated with cognitive deficits and depression severity in major depressive disorder. *J Psychiatr Res*, *84*, 9–17. doi:10.1016/j.jpsychires.2016.09.016
- Gong, Q. & He, Y. (2015). Depression, neuroimaging and connectomics: A selective overview. *Biol Psychiatry*, *77*(3), 223–35. doi:10.1016/j.biopsych.2014.08.009
- Grimm, O., Gass, N., Weber-Fahr, W., Sartorius, A., Schenker, E., Spedding, M., ... Meyer-Lindenberg, A. (2015). Acute ketamine challenge increases resting state prefrontal-hippocampal connectivity in both humans and rats. *Psychopharmacology (Berl)*. doi:10.1007/s00213-015-4022-y
- Grinsted, A., Moore, J. C., & Jevrejeva, S. (2004). Application of the cross wavelet transform and wavelet coherence to geophysical time series. *Non-linear Processes in Geophysics*, *11*(5/6), 561–566.
- Gudayol-Ferré, E., Peró-Cebollero, M., González-Garrido, A. A., & Guàrdia-Olmos, J. (2015). Changes in brain connectivity related to the treatment of depression measured through fMRI: A systematic review. *Frontiers in Human Neuroscience*, *9*(582). doi:10.3389/fnhum.2015.00582
- Guimerà, R., Mossa, S., Turtschi, A., & Amaral, L. A. N. (2005). The worldwide air transportation network: Anomalous centrality, community structure, and cities' global roles. *Proceedings of the National Academy of Sciences*, *102*(22), 7794–7799. doi:10.1073/pnas.0407994102
- Guo, J., Zhou, D., Grimm, S. W., & Bui, K. H. (2015). Pharmacokinetics, metabolism and excretion of [14C]-lanicemine (AZD6765), a novel low-trapping n-methyl-d-aspartic acid receptor channel blocker, in healthy subjects. *Xenobiotica*, *45*(3), 244–255. doi:10.3109/00498254.2014.966175
- Hikosaka, O., Bromberg-Martin, E., Hong, S., & Matsumoto, M. (2008). New insights on the subcortical representation of reward. *Curr Opin Neurobiol*, *18*(2), 203–8. doi:10.1016/j.conb.2008.07.002
- Höflich, A., Hahn, A., Küblböck, M., Kranz, G. S., Vanicek, T., Windischberger, C., ... Lanzenberger, R. (2015). Ketamine-induced modulation of the thalamo-cortical network in healthy volunteers as a model for schizophrenia. *International Journal of Neuropsychopharmacology*, *18*(9), pyv040. doi:10.1093/ijnp/pyv040
- Hwang, J. W., Xin, S. C., Ou, Y. M., Zhang, W. Y., Liang, Y. L., Chen, J., ... Kong, J. (2016). Enhanced default mode network connectivity with ventral striatum in subthreshold depression individuals. *J Psychiatr Res*, *76*, 111–20. doi:10.1016/j.jpsychires.2016.02.005



- 
- Hyvärinen, A., Karhunen, J., & Oja, E. (2001). Independent component analysis. Generic. John Wiley & Sons.
- Inta, D., Sartorius, A., & Gass, P. (2015). NMDA receptor blockade and catatonia: A complex relationship. *Schizophrenia Research*. doi:10.1016/j.schres.2015.07.029
- Jafri, M. J., Pearlson, G. D., Stevens, M., & Calhoun, V. D. (2008). A method for functional network connectivity among spatially independent resting-state components in schizophrenia. *NeuroImage*, *39*(4), 1666–1681. doi:10.1016/j.neuroimage.2007.11.001
- Johnson, K., Shah, A., Jaw-Tsai, S., Baxter, J., & Prakash, C. (2003). Metabolism, pharmacokinetics, and excretion of a highly selective n-methyl-d-aspartate receptor antagonist, traxoprodil, in human cytochrome P450 2D6 extensive and poor metabolizers. *Drug Metabolism and Disposition*, *31*(1), 76.
- Joules, R., Doyle, O. M., Schwarz, A. J., O'Daly, O. G., Brammer, M., Williams, S. C., & Mehta, M. A. (2015). Ketamine induces a robust whole-brain connectivity pattern that can be differentially modulated by drugs of different mechanism and clinical profile. *Psychopharmacology (Berl)*. doi:10.1007/s00213-015-3951-9
- Kaiser, M. & Varier, S. (2011). Evolution and development of brain networks: From caenorhabditis elegans to homo sapiens. *Network*, *22*(1-4), 143–7. doi:10.3109/0954898X.2011.638968
- Kelly, J., R. E., Alexopoulos, G. S., Wang, Z., Gunning, F. M., Murphy, C. F., Morimoto, S. S., . . . Hoptman, M. J. (2010). Visual inspection of independent components: Defining a procedure for artifact removal from fMRI data. *J Neurosci Methods*, *189*(2), 233–45. doi:10.1016/j.jneumeth.2010.03.028
- Khalili-Mahani, N., Niesters, M., van Osch, M. J., Oitzl, M., Veer, I., de Rooij, M., . . . Dahan, A. (2015). Ketamine interactions with biomarkers of stress: A randomized placebo-controlled repeated measures resting-state fMRI and PCASL pilot study in healthy men. *NeuroImage*, *108*, 396–409.
- Kranaster, L., Kammerer-Ciernioch, J., Hoyer, C., & Sartorius, A. (2011). Clinically favourable effects of ketamine as an anaesthetic for electroconvulsive therapy: A retrospective study. *European Archives of Psychiatry and Clinical Neuroscience*, *261*(8), 575–582. doi:10.1007/s00406-011-0205-7

- Långsjö, M. D. J., Kaisti, M. D. K., Aalto, M. S. S., Hinkka, P. L. S., Aantaa, M. D. R., Oikonen, M. S. V., ... Scheinin, M. D. H. (2003). Effects of subanesthetic doses of ketamine on regional cerebral blood flow, oxygen consumption, and blood volume in humans. *Anesthesiology*, *99*(3), 614–623.
- Latora, V. & Marchiori, M. (2001). Efficient behavior of small-world networks. *Phys Rev Lett*, *87*(19), 198701.
- Latora, V. & Marchiori, M. (2002). Is the boston subway a small-world network? *Physica A: Statistical Mechanics and its Applications*, *314*(1), 109–113. Horizons in Complex Systems. doi:10.1016/S0378-4371(02)01089-0
- Latora, V. & Marchiori, M. (2003). Economic small-world behavior in weighted networks. *The European Physical Journal B-Condensed Matter and Complex Systems*, *32*(2), 249–263.
- Liao, W., Ding, J., Marinazzo, D., Xu, Q., Wang, Z., Yuan, C., ... Chen, H. (2011). Small-world directed networks in the human brain: Multivariate Granger causality analysis of resting-state fMRI. *Neuroimage*, *54*(4), 2683–94. doi:10.1016/j.neuroimage.2010.11.007
- Liu, X., Hairston, J., Schrier, M., & Fan, J. (2011). Common and distinct networks underlying reward valence and processing stages: A meta-analysis of functional neuroimaging studies. *Neuroscience & Biobehavioral Reviews*, *35*(5), 1219–1236.
- Lu, H., Zou, Q., Gu, H., Raichle, M. E., Stein, E. A., & Yang, Y. (2012). Rat brains also have a default mode network. *Proc Natl Acad Sci U S A*, *109*(10), 3979–84. doi:10.1073/pnas.1200506109
- Luckenbaugh, D. A., Niciu, M. J., Ionescu, D. F., Nolan, N. M., Richards, E. M., Brutsche, N. E., ... Zarate, C. A. (2014). Do the dissociative side effects of ketamine mediate its antidepressant effects? *J Affect Disord*, *159*, 56–61. doi:10.1016/j.jad.2014.02.017
- Lv, Q., Yang, L., Li, G., Wang, Z., Shen, Z., Yu, W., ... Wang, Z. (2015). Large-scale persistent network reconfiguration induced by ketamine in anesthetized monkeys: Relevance to mood disorders. *Biol Psychiatry*. doi:10.1016/j.biopsych.2015.02.028
- McGirr, A., Berlim, M. T., Bond, D. J., Fleck, M. P., Yatham, L. N., & Lam, R. W. (2015). A systematic review and meta-analysis of randomized, double-blind, placebo-controlled trials of ketamine in the rapid treatment of major depressive episodes. *Psychological Medicine*, *45*(4), 693–704. doi:10.1017/S0033291714001603

- 
- Mealing, G. A. R., Lanthorn, T. H., Murray, C. L., Small, D. L., & Morley, P. (1999). Differences in degree of trapping of low-affinity uncompetitive n-methyl-d-aspartic acid receptor antagonists with similar kinetics of block. *Journal of Pharmacology and Experimental Therapeutics*, *288*(1), 204–210.
- Meibohm, B. & Derendorf, H. (1997). Basic concepts of pharmacokinetic/pharmacodynamic (PK/PD) modelling. *Int. Journal of Clinical Pharmacology and Therapeutics*, *35*(10), 401–413.
- Milgram, S. (1967). The small-world problem. *Psychology Today*, *1*(1), 61–67.
- Miller, O. H., Yang, L., Wang, C. C., Hargroder, E. A., Zhang, Y., Delpire, E., & Hall, B. J. (2014). GluN2B-containing NMDA receptors regulate depression-like behavior and are critical for the rapid antidepressant actions of ketamine. *Elife*, *3*, e03581. doi:10.7554/eLife.03581
- Mulders, P. C., van Eijndhoven, P. F., Schene, A. H., Beckmann, C. F., & Tendolkar, I. (2015). Resting-state functional connectivity in major depressive disorder: A review. *Neuroscience & Biobehavioral Reviews*, *56*, 330–344. doi:10.1016/j.neubiorev.2015.07.014
- Nasrallah, F. A., Tan, J., & Chuang, K.-H. (2012). Pharmacological modulation of functional connectivity:  $\alpha$ 2-adrenergic receptor agonist alters synchrony but not neural activation. *NeuroImage*, *60*(1), 436–446. doi:10.1016/j.neuroimage.2011.12.026
- Newman, M. E. J. (2004). Fast algorithm for detecting community structure in networks. *Phys. Rev. E*, *69*(6), 066133. doi:10.1103/PhysRevE.69.066133
- Niciu, M. J., Shovestul, B. J., Jaso, B. A., Farmer, C., Luckenbaugh, D. A., Brutsche, N. E., ... Zarate, J., C. A. (2018). Features of dissociation differentially predict antidepressant response to ketamine in treatment-resistant depression. *J Affect Disord*, *232*, 310–315. doi:10.1016/j.jad.2018.02.049
- Onnela, J.-P., Saramäki, J., Kertész, J., & Kaski, K. (2005). Intensity and coherence of motifs in weighted complex networks. *Physical Review E*, *71*(6). doi:10.1103/PhysRevE.71.065103
- Patel, A. X., Kundu, P., Rubinov, M., Jones, P. S., Vertes, P. E., Ersche, K. D., ... Bullmore, E. T. (2014). A wavelet method for modeling and despiking motion artifacts from resting-state fMRI time series. *Neuroimage*, *95*, 287–304. doi:10.1016/j.neuroimage.2014.03.012

- Posner, J., Cha, J., Wang, Z., Talati, A., Warner, V., Gerber, A., . . . Weissman, M. (2015). Increased default mode network connectivity in individuals at high familial risk for depression. *Neuropsychopharmacology*, *41*, 1759. doi:10.1038/npp.2015.342<https://www.nature.com/articles/npp2015342#supplementary-information>
- Power, J. D., Barnes, K. A., Snyder, A. Z., Schlaggar, B. L., & Petersen, S. E. (2012). Spurious but systematic correlations in functional connectivity mri networks arise from subject motion. *NeuroImage*, *59*(3), 2142–2154. doi:10.1016/j.neuroimage.2011.10.018
- Power, J., Cohen, A., Nelson, S., Wig, G., Barnes, K., Church, J., . . . Petersen, S. (2011). Functional network organization of the human brain. *Neuron*, *72*(4), 665–678.
- Power, J. D., Mitra, A., Laumann, T. O., Snyder, A. Z., Schlaggar, B. L., & Petersen, S. E. (2014). Methods to detect, characterize, and remove motion artifact in resting state fMRI. *NeuroImage*, *84*, 320–341. doi:10.1016/j.neuroimage.2013.08.048
- Preskorn, S. H., Baker, B., Kolluri, S., Menniti, F. S., Krams, M., & Landen, J. W. (2008). An innovative design to establish proof of concept of the antidepressant effects of the NR2B subunit selective n-methyl-d-aspartate antagonist, CP-101,606, in patients with treatment-refractory major depressive disorder. *J Clin Psychopharmacol*, *28*(6), 631–7. doi:10.1097/JCP.0b013e31818a6cea
- Pruim, R. H., Mennes, M., van Rooij, D., Llera, A., Buitelaar, J. K., & Beckmann, C. F. (2015). ICA-AROMA: A robust ica-based strategy for removing motion artifacts from fMRI data. *Neuroimage*, *112*, 267–77. doi:10.1016/j.neuroimage.2015.02.064
- Raichle, M. E., MacLeod, A. M., Snyder, A. Z., Powers, W. J., Gusnard, D. A., & Shulman, G. L. (2001). A default mode of brain function. *Proceedings of the National Academy of Sciences*, *98*(2), 676–682. doi:10.1073/pnas.98.2.676
- Reinwald, J. R., Becker, R., Mallien, A. S., Falfan-Melgoza, C., Sack, M., Clemm von Hohenberg, C., . . . Weber-Fahr, W. (2018). Neural mechanisms of early-life social stress as a developmental risk factor for severe psychiatric disorders. *Biological Psychiatry*, *84*(2), 116–128.
- Rolls, E. T. (2016). A non-reward attractor theory of depression. *Neurosci Biobehav Rev*, *68*, 47–58. doi:10.1016/j.neubiorev.2016.05.007

- 
- Rubinov, M. & Sporns, O. (2010). Complex network measures of brain connectivity: Uses and interpretations. *Neuroimage*, *52*(3), 1059–69. doi:10.1016/j.neuroimage.2009.10.003
- Rubinov, M. & Sporns, O. (2011). Weight-conserving characterization of complex functional brain networks. *Neuroimage*, *56*(4), 2068–79. doi:10.1016/j.neuroimage.2011.03.069
- Sabatinelli, D., Fortune, E. E., Li, Q., Siddiqui, A., Krafft, C., Oliver, W. T., ... Jeffries, J. (2011). Emotional perception: Meta-analyses of face and natural scene processing. *NeuroImage*, *54*(3), 2524–2533.
- Salvadore, G., Cornwell, B. R., Sambataro, F., Latov, D., Colon-Rosario, V., Carver, F., ... Zarate Jr, C. A. (2010). Anterior cingulate desynchronization and functional connectivity with the amygdala during a working memory task predict rapid antidepressant response to ketamine. *Neuropsychopharmacology*, *35*, 1415. doi:10.1038/npp.2010.24
- Sampath, D., Sathyanesan, M., & Newton, S. S. (2017). Cognitive dysfunction in major depression and alzheimer’s disease is associated with hippocampal-prefrontal cortex dysconnectivity. *Neuropsychiatr Dis Treat*, *13*, 1509–1519. doi:10.2147/NDT.S136122
- Sanacora, G., Smith, M. A., Pathak, S., Su, H. L., Boeijinga, P. H., McCarthy, D. J., & Quirk, M. C. (2014). Lanicemine: A low-trapping NMDA channel blocker produces sustained antidepressant efficacy with minimal psychotomimetic adverse effects. *Mol Psychiatry*, *19*(9), 978–85. doi:10.1038/mp.2013.130
- Sanacora, G., Zarate, C. A., Krystal, J. H., & Manji, H. K. (2008). Targeting the glutamatergic system to develop novel, improved therapeutics for mood disorders. *Nature Reviews Drug Discovery*, *7*, 426. doi:10.1038/nrd2462
- Satterthwaite, T. D., Kable, J. W., Vandekar, L., Katchmar, N., Bassett, D. S., Baldassano, C. F., ... Wolf, D. H. (2015). Common and dissociable dysfunction of the reward system in bipolar and unipolar depression. *Neuropsychopharmacology*, *40*, 2258. doi:10.1038/npp.2015.75
- Scheidegger, M., Henning, A., Walter, M., Boeker, H., Weigand, A., Seifritz, E., & Grimm, S. (2016). Effects of ketamine on cognition–emotion interaction in the brain. *NeuroImage*, *124*, 8–15. doi:10.1016/j.neuroimage.2015.08.070
- Scheidegger, M., Walter, M., Lehmann, M., Metzger, C., Grimm, S., Boeker, H., ... Seifritz, E. (2012). Ketamine decreases resting state functional network connectivity in healthy subjects: Implications for antidepressant drug action. *PLoS One*, *7*(9), e44799. doi:10.1371/journal.pone.0044799

- Scheinost, D., Holmes, S. E., DellaGioia, N., Schleifer, C., Matuskey, D., Abdallah, C. G., ... Esterlis, I. (2018). Multimodal investigation of network level effects using intrinsic functional connectivity, anatomical covariance, and structure-to-function correlations in unmedicated major depressive disorder. *Neuropsychopharmacology*, *43*(5), 1119–1127. doi:10.1038/npp.2017.229
- Schwarz, A. J., Danckaert, A., Reese, T., Gozzi, A., Paxinos, G., Watson, C., ... Bifone, A. (2006). A stereotaxic MRI template set for the rat brain with tissue class distribution maps and co-registered anatomical atlas: Application to pharmacological MRI. *NeuroImage*, *32*(2), 538–550. doi:10.1016/j.neuroimage.2006.04.214
- Schwarz, A. J., Gass, N., Sartorius, A., Risterucci, C., Spedding, M., Schenker, E., ... Weber-Fahr, W. (2013). Anti-correlated cortical networks of intrinsic connectivity in the rat brain. *Brain Connect*, *3*(5), 503–11. doi:10.1089/brain.2013.0168
- Schwarz, A. J., Gass, N., Sartorius, A., Zheng, L., Spedding, M., Schenker, E., ... Weber-Fahr, W. (2013). The low-frequency blood oxygenation level-dependent functional connectivity signature of the hippocampal-prefrontal network in the rat brain. *Neuroscience*, *228*, 243–58. doi:10.1016/j.neuroscience.2012.10.032
- Schwarz, A. J., Gozzi, A., & Bifone, A. (2009). Community structure in networks of functional connectivity: Resolving functional organization in the rat brain with pharmacological MRI. *NeuroImage*, *47*(1), 302–311.
- Schwarz, A. J. & McGonigle, J. (2011). Negative edges and soft thresholding in complex network analysis of resting state functional connectivity data. *Neuroimage*, *55*(3), 1132–46. doi:10.1016/j.neuroimage.2010.12.047
- Smucny, J., Wylie, K. P., & Tregellas, J. R. (2014). Functional magnetic resonance imaging of intrinsic brain networks for translational drug discovery. *Trends in Pharmacological Sciences*, *35*(8), 397–403.
- Soiza-Reilly, M. & Commons, K. G. (2011). Glutamatergic drive of the dorsal raphe nucleus. *J Chem Neuroanat*, *41*(4), 247–55. doi:10.1016/j.jchemneu.2011.04.004
- Sporns, O. (2011). *Networks of the brain*. MIT press.
- Sporns, O. (2013). Network attributes for segregation and integration in the human brain. *Curr Opin Neurobiol*, *23*(2), 162–71. doi:10.1016/j.conb.2012.11.015

- 
- Sporns, O. & Kotter, R. (2004). Motifs in brain networks. *PLoS Biol*, 2(11), e369. doi:10.1371/journal.pbio.0020369
- Spreng, R. N., Mar, R. A., & Kim, A. S. N. (2018). The common neural basis of autobiographical memory, prospection, navigation, theory of mind, and the default mode: A quantitative meta-analysis. *Journal of Cognitive Neuroscience*, 21(3), 489–510. doi:10.1162/jocn.2008.21029
- Stone, J. M. (2009). Imaging the glutamate system in humans: Relevance to drug discovery for schizophrenia. *Current Pharmaceutical Design*, 15(22), 2594–2602.
- Tang, H., Kukral, D., Li, Y.-W., Fronheiser, M., Malone, H., Pena, A., . . . Luo, F. (2018). Mapping the central effects of ( $\pm$ )-ketamine and traxoprodil using pharmacological magnetic resonance imaging in awake rats. *Journal of Psychopharmacology*, 32(2), 146–155. doi:10.1177/0269881117746901
- Taylor, T. J., Diringer, K., Russell, T., Venkatakrishnan, K., Wilner, K., Crownover, P. H., . . . Gibbs, M. A. (2006). Absolute oral bioavailability of traxoprodil in cytochrome P450 2D6 extensive and poor metabolizers. *Clinical Pharmacokinetics*, 45(10), 989–1001. doi:10.2165/00003088-200645100-00003
- van den Heuvel, M. P. & Hulshoff Pol, H. E. (2010). Exploring the brain network: A review on resting-state fMRI functional connectivity. *Eur Neuropsychopharmacol*, 20(8), 519–34. doi:10.1016/j.euroneuro.2010.03.008
- van Buuren, M., Gladwin, T. E., Zandbelt, B. B., van den Heuvel, M., Ramsey, N. F., Kahn, R. S., & Vink, M. (2009). Cardiorespiratory effects on default-mode network activity as measured with fMRI. *Human Brain Mapping*, 30(9), 3031–3042. doi:10.1002/hbm.20729
- Villar, M. J., Vitale, M. L., Hokfelt, T., & Verhofstad, A. A. (1988). Dorsal raphe serotonergic branching neurons projecting both to the lateral geniculate body and superior colliculus: A combined retrograde tracing-immunohistochemical study in the rat. *J Comp Neurol*, 277(1), 126–40. doi:10.1002/cne.902770109
- Vollenweider, F. X. & Kometer, M. (2010). The neurobiology of psychedelic drugs: Implications for the treatment of mood disorders. *Nat Rev Neurosci*, 11(9), 642–651. doi:10.1038/nrn2884
- Vuilleumier, P. (2015). Affective and motivational control of vision. *Curr Opin Neurol*, 28(1), 29–35. doi:10.1097/WCO.0000000000000159
- Watts, D. J. & Strogatz, S. H. (1998). Collective dynamics of ‘small-world’ networks. *Nature*, 393, 440. doi:10.1038/30918

- Williams, K. A., Magnuson, M., Majeed, W., LaConte, S. M., Peltier, S. J., Hu, X., & Keilholz, S. D. (2010). Comparison of  $\alpha$ -chloralose, medetomidine and isoflurane anesthesia for functional connectivity mapping in the rat. *Magn Reson Imaging*, *28*(7), 995–1003. doi:10.1016/j.mri.2010.03.007
- Zalesky, A., Fornito, A., & Bullmore, E. T. (2010). Network-based statistic: Identifying differences in brain networks. *NeuroImage*, *53*(4), 1197–1207. doi:10.1016/j.neuroimage.2010.06.041
- Zarate, C. A., Mathews, D., Ibrahim, L., Chaves, J. F., Marquardt, C., Ukoh, I., ... Luckenbaugh, D. A. (2013). A randomized trial of a low-trapping nonselective n-methyl-d-aspartate channel blocker in major depression. *Biological Psychiatry*, *74*(4), 257–264. doi:10.1016/j.biopsych.2012.10.019
- Zarate, C. A., Singh, J. B., Carlson, P. J., Brutsche, N. E., Ameli, R., Luckenbaugh, D. A., ... Manji, H. K. (2006). A randomized trial of an n-methyl-d-aspartate antagonist in treatment-resistant major depression. *Archives of General Psychiatry*, *63*(8), 856–864. doi:10.1001/archpsyc.63.8.856
- Zhang, J., Wang, J., Wu, Q., Kuang, W., Huang, X., He, Y., & Gong, Q. (2011). Disrupted brain connectivity networks in drug-naive, first-episode major depressive disorder. *Biol Psychiatry*, *70*(4), 334–42. doi:10.1016/j.biopsych.2011.05.018



# Curriculum Vitae

## Personal Data

**Name** Robert Becker  
**Date of birth** 10th December 1984  
**Place of birth** Wiesbaden  
**Marital status** not married  
**Nationality** German

## Scholar education

**1995 - 2001** Geschwister-Scholl-Gesamtschule, Wiesbaden  
**2001 - 2004** Carl-von-Ossietsky-Schule, Wiesbaden  
**23/06/2004** Abitur

## Academic studies

**2005 - 2012** Studies of physics (Diploma), Johannes-Gutenberg-Universität, Mainz  
**2011 - 2012** Diploma thesis „Erhöhung des NMR-Signals in Flüssigkeiten durch thermische Polarisation in gepulsten Magneten“  
**27/11/2012** Diploma  
**since 2013** PhD student, Research Group Translational Imaging, Department Neuroimaging, Central Institute for Mental Health, Mannheim

## Publications

### First authorships

Becker, R., Braun, U., Schwarz, A. J., Gass, N., Schweiger, J. I., Weber-Fahr, W., ... Meyer-Lindenberg, A. (2016). Species-conserved reconfigurations of brain network topology induced by ketamine. *Transl Psychiatry*, *6*, e786. doi:10.1038/tp.2016.53

Becker, R., Gass, N., Kußmaul, L., Schmid, B., Scheuerer, S., Schnell, D., ... Sartorius, A. (Submitted). NMDA receptor antagonists traxoprodil and lanicemine improve hippocampal-prefrontal coupling and reward related networks in rats. *Neuropsychopharmacology*.

### Co authorships

Artigas, F., Schenker, E., Celada, P., Spedding, M., Llado-Pelfort, L., Jurado, N., ... Schwarz, A. J. (2017). Defining the brain circuits involved in psychiatric disorders: IMI-NEWMEDS. *Nat Rev Drug Discov*, *16*(1), 1–2. doi:10.1038/nrd.2016.205

Bilbao, A., Falfán-Melgoza, C., Leixner, S., Becker, R., Singaravelu, S. K., Sack, M., ... Weber-Fahr, W. (2018). Longitudinal structural and functional brain network alterations in a mouse model of neuropathic pain. *Neuroscience*.

Clemm von Hohenberg, C., Weber-Fahr, W., Leibold, P., Ravi, N., Braun, U., Gass, N., ... Sartorius, A. (2018). Lateral habenula perturbation reduces default-mode network connectivity in a rat model of depression. *Translational Psychiatry*, *8*(1), 68. doi:10.1038/s41398-018-0121-y

Gass, N., Becker, R., Sack, M., Schwarz, A. J., Reinwald, J. R., Cosa-Linan, A., ... Sartorius, A. (2018). Antagonism at the NR2B subunit of NMDA receptors induces increased connectivity of the prefrontal and subcortical regions regulating reward behavior. *Psychopharmacology*, *235*(4), 1055–1068. doi:10.1007/s00213-017-4823-2

Gass, N., Becker, R., Schwarz, A. J., Weber-Fahr, W., Clemm von Hohenberg, C., Vollmayr, B., & Sartorius, A. (2016). Brain network reorganization differs in response to stress in rats genetically predisposed to depression and stress-resilient rats. *Translational Psychiatry*, *6*(12), e970. doi:10.1038/tp.2016.233

- Gass, N., Weber-Fahr, W., Sartorius, A., Becker, R., Didriksen, M., Stensbøl, T. B., ... Schwarz, A. J. (2016). An acetylcholine alpha7 positive allosteric modulator rescues a schizophrenia-associated brain endophenotype in the 15q13.3 microdeletion, encompassing CHRNA7. *European Neuropsychopharmacology*, *26*(7), 1150–1160. doi:10.1016/j.euroneuro.2016.03.013
- Reinwald, J. R., Becker, R., Mallien, A. S., Falfan-Melgoza, C., Sack, M., Clemm von Hohenberg, C., ... Weber-Fahr, W. (2018). Neural mechanisms of early-life social stress as a developmental risk factor for severe psychiatric disorders. *Biological Psychiatry*, *84*(2), 116–128.
- Tollens, F., Gass, N., Becker, R., Schwarz, A. J., Risterucci, C., Künnecke, B., ... Sartorius, A. (2018). The affinity of antipsychotic drugs to dopamine and serotonin 5-HT2 receptors determines their effects on prefrontal-striatal functional connectivity. *European Neuropsychopharmacology*. doi:10.1016/j.euroneuro.2018.05.016



# Acknowledgements

First of all, I thank my supervisor Prof. Dr. Alexander Sartorius as well Dr. Wolfgang Weber-Fahr and Prof. Dr. Gabi Ende for the opportunity to conduct the research which lead to this thesis and their guidance and advice, I could always rely on.

I am especially thankful to Dr. Natalia Gass for her valuable cooperation on nearly every project I worked on over the last years, including those presented here.

To Dr. Urs Braun I owe sincere thanks for the collaboration on the ketamine study.

All of my colleagues at the research group Translational Imaging and the department Neuroimaging deserve my deepest gratitude for making this group such a great place to work at. Thanks to Dr. Markus Sack, Felix Hörner, Dr. Wolfgang Weber-Fahr, Dr. Alejandro Cosa-Linan, Dr. Jonathan Reinwald, Claudia Falfan-Melgoza, and Dr. Guoying Wang (to name but a few) for five years of excellent collaboration, many hours of interesting discussion, countless lunch and cigarette breaks, and a lot of fun.

Outside of the scientific world, I first have to thank my family, especially my parents Lis and Carl, without whose lifelong support, this work would not have been possible.

I also thank the archery division of the SG 1744 Mannheim for offering frequent and valuable distraction.

Finally, I am very grateful to my friends Teresa, Ranya, Achim, Frieder and Jannis for always supporting me, listening to my complaints and simply being there whenever I feel like leaving town for a few days.